Input impedance of the cochlea in cat[a)]

Thomas J. Lynch, III,[b)] Victor Nedzelnitsky,[c)] and William T. Peake
Department of Electrical Engineering and Computer Science and Research Laboratory of Electronics, Massachusetts Institute of Technology, Cambridge, Massachusetts 02139 and Eaton–Peabody Laboratory of Auditory Physiology, Massachusetts Eye and Ear Infirmary, Boston, Massachusetts 02114

(Received 24 June 1981; accepted for publication 17 March 1982)

Tones were delivered directly to the stapes in anesthetized cats after removal of the tympanic membrane, malleus, and incus. Measurements were made of the complex amplitudes of the sound pressure on the stapes P_S, stapes velocity V_S, and sound pressure in the vestibule P_V. From these data, acoustic impedance of the stapes *and* cochlea $Z_{SC} \triangleq P_S/U_S$, and of the cochlea alone $Z_C \triangleq P_V/U_S$ were computed ($U_S \triangleq$ volume velocity of the stapes $= V_S \times$ area of the stapes footplate). Some measurements were made on modified preparations in which (1) holes were drilled into the vestibule and scala tympani, (2) the basal end of the basilar membrane was destroyed, (3) cochlear fluid was removed, or (4) static pressure was applied to the stapes. For frequencies between 0.5 and 5 kHz, $Z_{SC} \cong Z_C$; this impedance is primarily resistive ($|Z_C| \cong 1.2 \times 10^6$dyn-s/cm^5) and is determined by the basilar membrane and cochlear fluids. For frequencies below 0.3 kHz, $|Z_{SC}| > |Z_C|$ and Z_{SC} is primarily determined by the stiffness of the annular ligament; drying of the ligament or changes in the static pressure difference across the footplate can produce large changes in $|Z_{SC}|$. For frequencies below 30 Hz, Z_C is apparently controlled by the stiffness of the round-window membrane. All of the results can be represented by an network of eight lumped elements in which some of the elements can be associated with specific anatomical structures. Computations indicate that for the cat the sound pressure at the input to the cochlea at behavioral threshold is constant between 1 and 8 kHz, but increases as frequency is decreased below 1 kHz. Apparently, mechanisms within the cochlea (or more centrally) have an important influence on the frequency dependence of behavioral threshold at low frequencies.

PACS numbers: 43.63.Kz, 43.66.Gf, 43.80,Lb, 43.63.Hx

INTRODUCTION

Airborne acoustic signals are normally transmitted from the external ear canal to the cochlea through the mechanical system of the middle ear. To understand the operation of the middle ear, it is necessary to know the mechanical constraints imposed by the cochlea on the relation between force and motion at the oval window. If the stapes motion is one dimensional and the system is linear, these constraints are characterized by the "input impedance" of the cochlea, which represents the mechanical "load" driven by the middle ear. To understand the quantitative variations of middle-ear response among individuals and species we also need to know how the mechanical properties of various anatomical structures contribute to the cochlear input impedance.

Some measurements of cochlear input impedance have been reported for cats (Tonndorf *et al.*, 1966; Khanna and Tonndorf, 1971) and for human cadavers (Békésy, 1942, 1960, pp. 435–436; Onchi, 1961). All of these results are seriously limited in their accuracy by technical problems in the measurements. Recently measurements of intracochlear sound pressure have been combined with measurements of ossicular motion to estimate cochlear input impedance for the cat (Nedzelnitsky, 1974a, b, 1980) and guinea pig (Franke and Dancer, 1980). The primary goal of the work reported here is to contribute to a more complete understanding of the middle ear by measuring the impedances of the cochlea and stapes in the cat and by determining experimentally how various anatomical structures influence these impedances.

I. MECHANICAL MODEL AND DEFINITION OF VARIABLES

Acoustic stimulation at the tympanic membrane produces pistonlike motion of the stapes (Guinan and Peake, 1967; Dankbaar, 1970; Høgmoen and Gundersen, 1977; Rhode, 1978). The forces that act on the stapes result from the structures adjoining it and from the sound pressures in the middle-ear cavity and the vestibule (Fig. 1). If we assume that (1) the stapes is a rigid body and (2) each of the pressures p_S and p_V is uniform over the relevant surface, then summation of the force components that are along the direction of motion yields

$$A_{fp}p_S + f_J = f_{AL} + A_{fp}p_V + M_S^m \dot{v}_S, \quad (1)$$

where

A_{fp} = effective area of the stapes footplate,[1]

M_S^m = (mechanical) mass of the stapes, and

$\dot{v}_S = dv_S/dt$ = acceleration of the stapes.

If we further assume that this system is linear for the small displacements associated with acoustic stimulation,

[a)] A portion of this work was submitted by T. J. Lynch, III as a master's thesis to the Department of Electrical Engineering and Computer Science, Massachusetts Institute of Technology, September 1974 and a preliminary presentation was given at the 91st meeting of the Acoustical Society of America (Lynch *et al.*, 1976).

[b)] Present address: M.I.T. Lincoln Laboratory, Room L-110, Lexington, MA 02173.

[c)] Present address: National Bureau of Standards, Sound Building (233), Room A149, Washington, DC 20234.

 0001-4966/82/070108-23$00.80

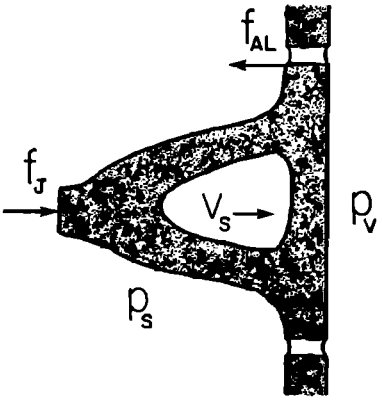

FIG. 1. Diagram indicating pressures and forces acting on the stapes and the resulting stapes motion. p_S = sound pressure on the middle-ear surface of the stapes, p_V = sound pressure on the vestibular surface, f_J = force from the incudo-stapedial joint, f_{AL} = force from the annular ligament, and v_S = velocity of the stapes. Forces perpendicular to the assumed direction of motion, including that from the stapedius tendon, have been omitted.

then for the sinusoidal steady state (of angular frequency ω) the variables can be represented by their complex amplitudes $P_S, P_V, F_J, F_{AL}, V_S$; the forces of the annular ligament and cochlea can be expressed in terms of impedances with $F_{AL} \triangleq Z^m_{AL} V_S$ and $A_{fp} P_V \triangleq Z^m_C V_S$, where Z^m_{AL} and Z^m_C are the mechanical impedances [force/(lineal velocity)] due to the annular ligament and cochlea, respectively. With these substitutions Eq. (1) can be rearranged to give

$$(A_{fp} P_S + F_J)/V_S = Z^m_{AL} + j\omega M^m_S + Z^m_C = Z^m_S + Z^m_C, \quad (2)$$

where we have defined $Z^m_S \triangleq Z^m_{AL} + j\omega M^m_S$. Division of Eq. (2) by A^2_{fp} yields

$$(P_S + F_J/A_{fp})/U_S = Z^a_S + Z^a_C \triangleq Z^a_{SC}, \quad (3)$$

where

$U_S = A_{fp} V_S$ = complex amplitude of stapes *volume* velocity,

$Z^a_S \triangleq Z^m_S / A^2_{fp}$ = *acoustic* impedance of the stapes (and annular ligament),

$Z^a_C \triangleq Z^m_C / A^2_{fp}$ = *acoustic* impedance of the cochlea, and

Z^a_{SC} = *acoustic* impedance of the stapes *and* cochlea.

In the rest of this paper we will deal exclusively with *acoustic* impedances and the superscripts in Z^a_C, etc., will be omitted.

II. METHODS

A. General plan of the measurements

Equation (3) indicates that the stapes can be driven both by force applied from the incus F_J and by sound pressure applied to the stapes surface P_S. In the experiments reported here most of the middle-ear structures were removed and acoustic stimuli were delivered to a cavity around the stapes (Fig. 2) so that $F_J = 0$ and P_S is the sole driving variable. This method, which has been used previously (Wever and Lawrence, 1950; Tonndorf *et al.*, 1966; Khanna and Tonndorf, 1971), has the advantages that no rigid mechanical attachment need be made to the stapes and that the driving force can be inferred from measurements of sound pressure

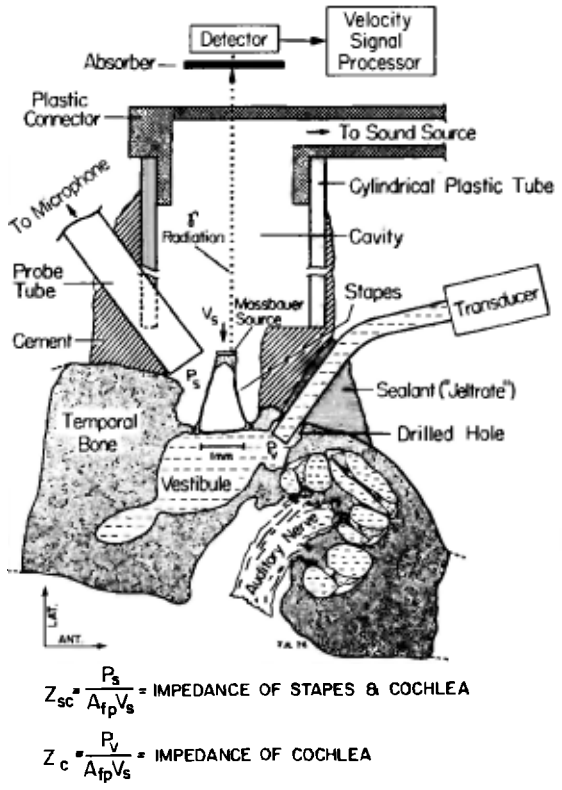

FIG. 2. Configuration of the measurement systems. The sound pressure on the lateral side of the stapes P_S was measured with an air-filled probe-tube microphone system (left side). The lineal velocity of the stapes V_S was measured using the Mössbauer technique, in which a gamma-ray source is attached to the stapes and the rate at which photons are detected through a resonant absorber is used to determine the velocity. Sound pressure on the medial side of the stapes P_V was measured with a transducer (right side) having a fluid-filled probe tube that was introduced into the vestibule through a hole drilled into the temporal bone. The lower portion of the figure was traced from a projection of a histological section of the temporal bone of one of the experimental cats. (The section was approximately in a horizontal plane, but was slightly inclined so as to intersect both the stapes footplate and the drilled hole.) The probe tubes and acoustic cavity around the stapes are drawn approximately to scale, but their locations have been distorted to present a clearer picture in two dimensions.

made with a probe-tube microphone. From measurements of the three complex amplitudes P_S, P_V, and V_S and of the stapes footplate area A_{fp}, the acoustic impedances can be calculated as $Z_{SC} = P_S/(A_{fp} V_S)$ and $Z_C = P_V/(A_{fp} V_S)$.

B. Animal preparation

Adult cats weighing between 1.6 and 3.9 kg were initially anesthetized with an intraperitoneal injection of Dial (0.75 ml/kg). Additional doses of 0.2 ml were administered as needed. Each cat received 250 000 units of penicillin intramuscularly and 50 ml of physiological saline subcutaneously. A cannula was inserted into the trachea. Rectal temperature was monitored and maintained at 37° ± 2° C with a heating pad.

The pinna, ear canal, tympanic membrane, bulla wall, bony septum, and ventral segment of the tympanic ring were removed to expose the middle ear. The incus was then separated from the stapes at the incudo-stapedial joint with a miniature scalpel. The tensor-tympani tendon was cut, and the remaining segment of the tympanic ring, the malleus, and the incus were removed.

In order to provide an unobstructed view of the stapes footplate some nearby structures were removed. The tensor tympani was completely excised. The stapedius tendon was severed near its point of attachment to the stapes. (Measurements of $|Z_{SC}|$ in one cat before and after stapedius detachment showed no significant changes.) Usually the bone covering the facial-nerve canal posterodorsal to the stapes was removed along with a short section of the facial nerve. Both ends of the canal were then plugged with cotton to restrict fluid seepage. The stapedius muscle was also removed. During these procedures it was important to avoid breaking into the lateral semicircular canal.

To provide a good surface for secure bonding of cement, the periosteum was removed from the petrous bone surrounding the oval window and the exposed bone was allowed to dry. A few drops of physiological saline solution were placed around the stapes footplate to keep the annular ligament moist (see Sec. III).

A cavity was then constructed around the stapes (Fig. 2). The base of the cavity was made with dental cement ("Grip," S. S. White Co.) which was applied to the dry bone surrounding the oval window so as to fill the spaces formed by the removal of the facial nerve and stapedius and tensor-tympani muscles. Thin layers of the cement were built up to form a flat surface around the oval window. During this process the end of the P_S probe tube was positioned less than 2 mm from the dorsal edge of the stapes footplate and the cement cavity wall was built around the tube. A cylindrical, rigid, plastic tube (3 mm i.d., 7 mm long) was then cemented to the base to form a cavity containing the stapes and one end of the probe tube. The Mössbauer source was affixed to the stapes head using either petrolatum or zinc-oxide cement.

Usually after this portion of the procedure had been completed, we connected the sound source to the cavity and made initial measurements of pressure P_S and velocity V_S. These measurements included determination of the stimulus level $|P_S|$ required to produce a constant velocity amplitude over a range of stimulus frequency f so that $|Z_{SC}(f)|$ could be estimated.

C. Stimulus generation and measurement

Rapid measurement of stapes velocity with the Mössbauer method requires high sound-pressure levels at the stapes. The stimulus system consisted of an oscillator, attenuator, power amplifier, and either a Jensen DD-100 or an Atlas PD-60 driver coupled to the stapes cavity with rigid plastic tubing. This system could produce up to 150 dB SPL from 20 to 5000 Hz. For some of the measurements the oscillator and attenuator were controlled by a computer system which allowed sweeping of the frequency while keeping either a stimulus or response variable constant (Weiss *et al.*, 1969).

The microphone (12 mm diam Brüel & Kjaer 4134) and probe tube used for P_S measurements were calibrated (Weiss and Peake, 1972) in a specially constructed cavity. A condenser microphone (25 mm B&K 4132) was used as a sound source to drive a cylindrical cavity 3 mm in diameter and 7 mm long. A calibrated condenser microphone (3 mm B&K 4138) terminated this cavity and the probe tube was inserted so that its tip was 1.5 mm from the center of the microphone diaphragm. A theoretical analysis indicates that the sound pressures at the probe tip and at the microphone diaphragm differ by less than 1 dB for frequenices below 17 kHz. The calibration curve was stored in the computer system so that output voltages from the probe-tube microphone could be converted to sound pressures.

In one experiment static pressure was also introduced into the cavity around the stapes. An otoadmittance meter (Grason–Stadler 1720) was used as the static pressure source and connected by a T junction to our sound delivery tube. A special housing for the P_S condenser microphone vented the static pressure to the back side of the diaphragm so that the microphone sensitivity was nearly independent of static pressure.

D. Velocity measurements

1. Introduction

Our use of the Mössbauer effect for velocity measurements differs somewhat from the methods of other groups (Gilad *et al.*, 1967; Johnstone *et al.*, 1970; Rhode, 1971; Helfenstein, 1974; Gundersen *et al.*, 1978). Figure 3 shows the relation of the photon rate at the detector to the velocity of the Mössbauer source. This relation can be expressed as

$$r = R_\infty (1 - a/\{1 + [(v - V_i)/\Gamma]^2\}), \tag{4}$$

where

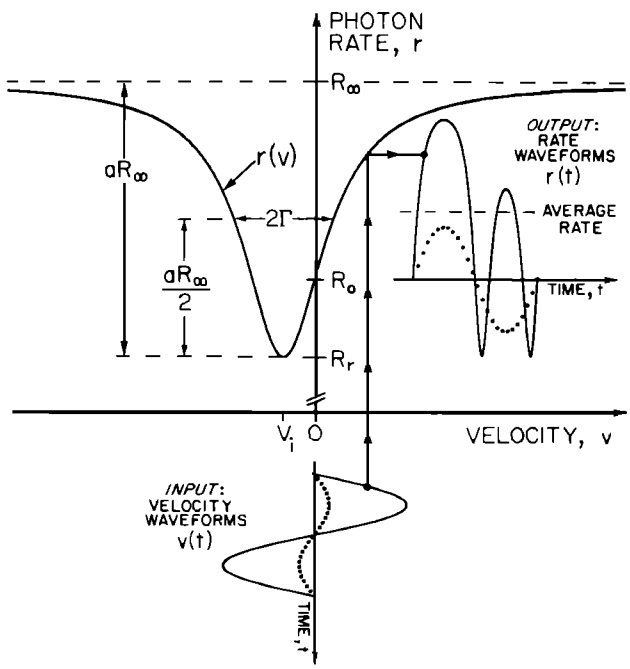

FIG. 3. Essential features of the Mössbauer method for measurement of velocity. The curve $r(v)$, represents the dependence of photon detection rate r on velocity v. Two sinusoidal velocity waveforms and the resulting rate waveforms are shown. The smaller velocity waveform (peak amplitude = 0.5 $|V_i|$: dotted curve) produces a rate waveform that is approximately sinusoidal with an average value about equal to R_0, the rate with $v = 0$. The larger velocity waveform (peak amplitude = 3 $|V_i|$: solid curve) produces a nonsinusoidal rate waveform with an average value (indicated by the dashed line) that is larger than the resting rate R_0. (Positive velocity indicates motion of the Mössbauer source toward the stationary absorber.)

r = detected photon rate (counts/s),
R_∞ = asymptotic value of r when $|v - V_i| \gg \Gamma$,
a = fractional effect = $(R_\infty - R_r)/R_\infty$, where
R_r = minimum (resonant) rate,
v = velocity of the Mössbauer source,
V_i = isomer shift (velocity for maximum absorption), and
Γ = linewidth (or half-width at half-height).

The relation between r and v is determined by four parameters R_∞, V_i, a, and Γ, which must be known to determine v from measurements of r. R_∞ depends on the size and specific activity of the source and on the configuration of the absorber and detector (e.g., source-to-detector distance, detector size, and efficiency). V_i is determined by the source and absorber materials. Γ and a are primarily determined by the materials and configuration of the source and absorber, but they can also be influenced by materials between the radioactive substance and the absorber (e.g., source matrix material, acoustic cavity walls, bone, fluid) and by the photon detection scheme (e.g., the width of the pulse-height window).

Use of nonzero isomer shift has two advantages. (1) As the velocity decreases, the sensitivity $\Delta r/\Delta v$ does not approach zero (as it does if $V_i = 0$). (2) Positive and negative velocity can be distinguished, thereby avoiding a "180° ambiguity in phase" (Johnstone and Sellick, 1972, p. 7; Robles *et al.*, 1976, p. 929).

We used two procedures to measure velocity. (1) The velocity waveform $v(t)$ was obtained from the instantaneous rate $r(t)$. (2) For sinusoidal waveforms the velocity magnitude $|V|$ was obtained from the average rate $\overline{r(t)}$.

2. Velocity waveforms

Equation (4) can be solved for v to give

$$v/V_i = 1 \pm [(R_\infty - R_0)(r - R_r)/(R_0 - R_r)(R_\infty - r)]^{1/2}. \quad (5)$$

If the four parameters R_r, R_0, R_∞, and V_i are known, measurements of $r(t)$ can be converted to $v(t)$ by Eq. (5) except for the ambiguity associated with the sign of the square root. This ambiguity was avoided by contraining the stimulus to levels such that $|v| < |V_i|$, which ensures that the sign of the square root in Eq. (5) is negative.

Our method of determining velocity *waveforms* was basically that used by Gilad *et al.* (1967). We used a laboratory computer system to (a) accumulate photon counts synchronized to the stimulus cycles, (b) perform the computation of Eq. (5), and (c) display a velocity waveform (Lewis and Peake, 1971).

To calibrate this sytem R_0, R_r, and R_∞ were measured in each experiment with the source, absorber, and detector in place. R_0 was measured with no stimulus. A stimulus level high enough to drive $|v| > |V_i|$ was then used to estimate R_r from minima of $r(t)$ (see solid waveform in Fig. 3). An even higher stimulus level was used to estimate R_∞ from maxima of $r(t)$. After completion of this calibration procedure, waveforms of $v(t)/V_i$ were computed according to Eq. (5) as illustrated in Fig. 4. For sinusoidal stimuli the magnitude and

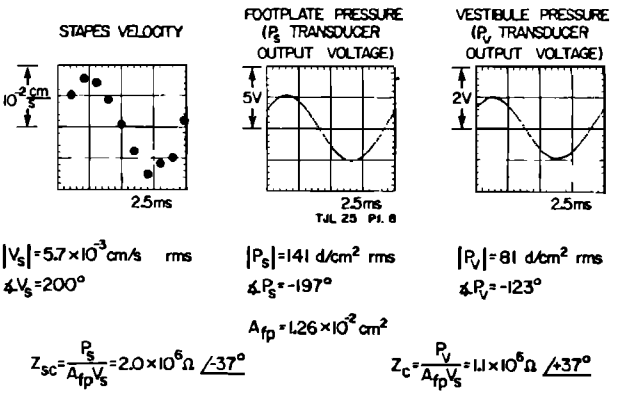

FIG. 4. Examples of averaged waveforms of response variables and impedance computations. In the velocity waveform, negative v_S is upwards. The other two waveforms are the amplified voltages from the two pressure transducers; pressures are computed by taking into account the transfer functions of the transducers and amplifiers. The angles shown for V_S, P_S, and P_V are relative to the electric input to the stimulus system. Impedances are computed from the fundamental components of the waveforms. This velocity waveform (ten points/period) was computed over 63 846 periods; about 5 min were required to obtain this waveform. The pressure waveforms (100 points/period) were averaged for 1000 periods; about 5 s were required to obtain each of these waveforms. Stimulus frequency = 0.4 kHz.

angle of the fundamental, second, and third harmonic components of the waveforms were computed.

The time required to make a velocity measurement by this method is primarily determined by the random process associated with the emission of photons. The measured rate, which is an estimate of the instantaneous rate of the random process, is a random variable; to increase the accuracy of the estimate, the photon counts are averaged over many stimulus repetitions. The variability in the velocity estimate is a function of the velocity magnitude, the photon rate, and the averaging time.

The limitations of the "velocity waveform" method can be illustrated by considering the time required to make a particular measurement. With our Mössbauer source of ^{57}Co in palladium and a stainless steel absorber enriched in ^{57}Fe we obtained parameter values of $V_i = -0.2$ mm/s, $\Gamma = 0.3$ mm/s, and $a = 0.3$. The detector was usually placed so as to give $R_0 \cong 10^3$/s. For sinusoids with peak amplitude near 0.5 V_i a few minutes of averaging was required to obtain relatively clear velocity waveforms (e.g., Fig. 4) with a resolution of ten points per stimulus cycle. Since peak amplitudes greater than $|V_i|$ produced the ambiguity mentioned above (and large errors because of the relative insensitivity of rate to velocity for $|v - V_i| \gg \Gamma$), it was undesirable to work at larger velocities. Smaller velocities required longer averaging times so we usually made velocity measurements (magnitude and angle) at only one level (ca. 0.5 $|V_i|$ peak amplitude). Obtaining velocity waveforms at 20 frequencies with the associated p_V and p_S waveforms took approximately 10 h.

3. Velocity magnitude from average rate

The mean rate, $\overline{r(t)}$, can be estimated more rapidly than the waveform $r(t)$. If $v(t) = \sqrt{2}V \sin(\omega t)$, integration of Eq. (4) yields

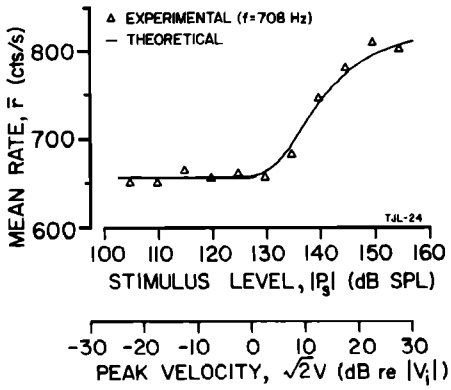

FIG. 5. Mean photon rate (counts/s) versus stimulus and velocity level. The theoretical curve ($\bar{r}$ vs peak velocity, $\sqrt{2}V$) was determined from Eq. (6) using parameter values ($R_r = 595$, $R_0 = 658$, $R_\infty = 820$ counts/s) that were measured during an experiment. The experimental points are measured mean rate versus stimulus sound-pressure level. The two plots were positioned horizontally so as to minimize the mean square error between experimental and theoretical points. $|V_i| = 0.2$ mm/s.

$$\bar{r} = R_\infty \{1 - a[(y + x^{1/2})/2x]^{1/2}\}, \qquad (6)$$

where $x = y^2 + b$, $y = [(2V^2 - V_i^2)/\Gamma^2] + 1$, and $b = (2V_i/\Gamma)^2$. From Eq. (6) we find (Fig. 5) that $\bar{r}$ increases from R_0 to close to R_∞ when $|\sqrt{2}V/V_i|$ increases from 0 to 30 dB. For $|\sqrt{2}V/V_i|$ in the range 10 to 20 dB, $\bar{r}$ is a sensitive indicator of the velocity amplitude. To determine impedance magnitude over a wide frequency range, it is convenient to adjust the stimulus level at each frequency so that the velocity remains in the range where $\bar{r}$ is sensitive to changes in $|V|$. The computer system was programmed to adjust the stimulus level so that the measured value of $\bar{r}$ was within a given tolerance of a specified value and to display the resulting stimulus level versus frequency. The curve representing Eq. (6) was used to convert the specified value of $\bar{r}$ into a velocity magnitude (Fig. 5) so that impedance magnitude could be computed.

The photon rate was averaged with a "rate meter" having a time constant of 0.5 s. With this computerized sweep system we could make measurements at 20 frequencies (between 30 and 10 000 Hz) in 5 min.

4. Determination of isomer shift V_i

Both the velocity-waveform and mean-rate measurements produced velocity values expressed in terms of the isomer shift V_i. To determine the value of V_i we measured the magnitude of the motion of a vibrator at one frequency (56 Hz) (1) with the Mössbauer waveform method, (2) with a calibrated accelerometer, and (3) with a microscope, eyepiece micrometer, and stroboscopic illumination. The latter two measures agreed within 20%. To make the Mössbauer waveform magnitude equal to the average of the other two measures required that $V_i = -0.2$ mm/s.

5. Validation of the method

The system was tested by measuring velocity waveforms on a vibrator (B&K 4290 or 4810) for sinusoidal motion at frequencies from 30 to 30 000 Hz. The Mössbauer source was attached to an accelerometer with petrolatum. Mössbauer measurements were compared with those obtained from the accelerometer. These measurements agreed (within $\pm$ 2.5 dB and $\pm$ 15°) indicating that a thin layer of petrolatum was a suitable adhesive for the Mössbauer source. A similar test of the constant $\bar{r}$ method from 10 to 20 000 Hz demonstrated the same accuracy in velocity magnitude. To further test the adhesion (in three cats) a Mössbauer source was attached to the head of the stapes first with petrolatum and then with zinc-oxide dental cement; measurements of $|Z_{SC}|$ were not significantly different. Since the cement bonds the source to the stapes very rigidly, this result indicates that the petrolatum is also an adequate bonding agent and has the advantage of ease in placement and removal.

The Mössbauer source was made (New England Nuclear) from ^{57}Co plated on palladium foil (12 μm thick). A rectangular piece (300 × 380 μm) was cut to fit on the head of the stapes. The estimated mass of the source (20 μg) is about 4% of the stapes mass (see Sec. III D*1*). Since the stapes mass itself seems to make only a small contribution to the normal Z_{SC}, the addition of the source mass should have a negligible effect.

The Mössbauer system detects the velocity of the source relative to the absorber. For determination of the impedances Z_{SC} and Z_C we need to know the velocity of the stapes relative to the skull (petrous bone). To test whether the velocity of either the petrous bone or the absorber was significantly different from zero, in one preparation the Mössbauer source was placed on the petrous bone adjacent to the oval window. With the highest sound pressures that our acoustic system could generate, we looked for increases in $\bar{r}$ at frequencies spanning the range that we used. We were unable to detect any motion with this method. Since the same method was able to produce increases in $\bar{r}$ at lower sound pressures when the source was on the stapes, the motion of the other structures, such as skull or absorber, was negligible.

6. Summary of velocity measurement methods

The ranges of velocity and frequency over which these two methods were applied are indicated in Fig. 6 along with a curve indicating an upper limit for predominantly linear behavior of the intact ossicular chain. The figure shows that the velocity levels used in the work reported here were within the range in which the fundamental component of the motion shows linear growth with stimulus level, with the possible exception of the $\bar{r}$ measurements at the lowest frequencies.

E. Measurement of sound pressure in the vestibule

The transducers used for measuring intracochlear pressure and their calibration have been described by Nedzelnitzky (1974a, 1980).

1. Calibration

A fluid-filled vial was mounted on a vibrator to generate an approximately uniform pressure field for calibration purposes. The tip of the transducer's probe tube and a refer-

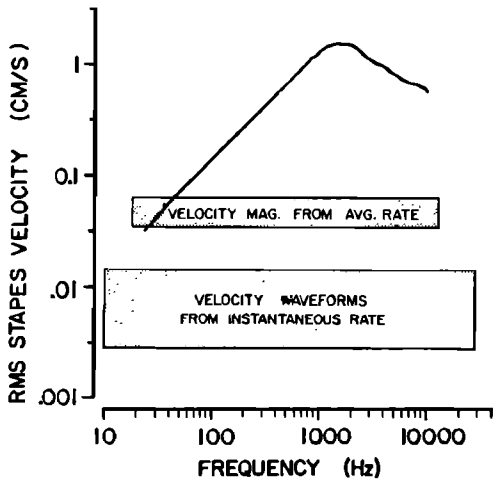

FIG. 6. Ranges of the two velocity measurement methods compared with an estimate of the linear range of operation for the intact ossicular chain. The velocity and frequency ranges used for each measurement method are indicated by the shaded rectangles. The curve (based on an average transfer function of the cat's middle ear, Guinan and Peake, 1967) gives the stapes velocity for a sound pressure of 130 dB SPL at the tympanic membrane (with the bulla open and the bony septum removed). The results of Guinan and Peake (1967) indicated that the fundamental component of stapes displacement is a linear function of stimulus sound-pressure level at least up to this pressure level. In this and all the following figures the ordinate is logarithmic with tick marks at equal logarithmic intervals.

ence transducer were immersed in the fluid to the same depth and the outputs of both were measured to determine a calibration curve for the probe-tube transducer. [The reference transducer, which had an exposed diaphragm, was calibrated in air using an electrostatic actuator and pistonphone (Brüel, 1964, 1965).] At the high frequencies this method is more accurate than the method reported previously (Nedzelnitsky, 1980), because it does not require absolute rigidity of the attachment of the vial to the vibrator.

The probe was calibrated at the beginning and end of each experiment. In general, measurements are reported only for frequencies where these two calibrations agreed within $\pm$ 5 dB. (The largest differences usually occurred at high frequencies and the low-frequency differences were considerably smaller.) In order to confirm that the transducer was responding to the pressure at the probe tip, the tip was plugged at the end of the experiment and measurements in the vial were repeated. The output measurement was considered valid only when it was at least 10 dB larger than the "plugged-tip" output. This criterion usually limited the P_V measurements to frequencies below 10 kHz.

2. Transducer placement

Prior to the insertion of the P_V pressure probe, a hole (usually about 0.3 mm diam) was drilled into the vestibule anteroventrally to the oval window. Perilymph always flowed from the open hole. If there was bleeding from the vestibule, physiological saline was used to wash away the blood before it clotted. (To determine whether the drilling produced gross disruptions in the labyrinth, temporal bones from four experiments were prepared for histological sections. In each case there was a clean hole in the bone without apparent damage to the annular ligament or the basilar membrane.) With the P_V pressure transducer mounted on a micromanipulator the probe tube was inserted into the hole. To provide a seal around the probe tube a mixture of alginate-base dental impression material ("Jeltrate," L. D. Caulk Co.) was placed on the bone around the probe tube. This liquid set within a few minutes into a firm gel which provided a seal that prevented perilymph leakage around the probe tube.

Measurements of $|Z_{SC}|$ were used to test the quality of the seal (e.g., Fig. 9). If $|Z_{SC}|$ was not the same (within a few dB) with the hole sealed as it had been with the labyrinth intact, the Jeltrate was removed, the bone around the hole was dried, and another application was tried. In most cases it was possible to achieve a good seal that was stable for at least a few hours.

3. Validity of measurements

In order to ensure that the transducer was measuring the pressure at the tip of the probe tube, measurements were made in the vestibule (in two cats) before and after the probe tip was mechanically plugged. Also, the output of the measuring system (the noise floor) was determined with the stimulus off. For all results reported here the measurements are *at least* 10 dB above both the noise floor and the plugged-tip output.

F. Impedance computations and accuracy

To calculate acoustic impedances from the pressure and velocity measurements, the stapes footplate area A_{fp} must be known. The area of the oval window was measured in temporal bones of eight of the cats used in experiments. A mean of 1.20 mm^2 was obtained with a range of 1.00 to 1.38 mm^2 and a standard deviation of 0.13 mm^2. Similar results have been reported by Wever *et al.* (1948) and Guinan and Peake (1967). In the results presented here the footplate area was taken (somewhat arbitrarily) as 1.26 mm^2 in all impedance calculations. We estimate that errors in acoustic impedance magnitude of approximately $\pm$ 1.5 dB may be introduced by ignoring intercat variations of A_{fp}.

Z_C and Z_{SC} were calculated from data obtained with both of the velocity measurement methods described above. Based on worst-case esimates of errors in the quantities used (A_{fp}, $\pm$ 1.5 dB; $|P_S|$, $\pm$ 1.5 dB; $|V_S|$, $\pm$ 3 dB) we calculate the *limits* on error in $|Z_{SC}|$ as $\pm$ 6 dB with the waveform method. Because of larger inaccuracy in absolute calibration and instability in the P_V transducer, we estimate the error limits in $|Z_C|$ as $\pm$ 10 dB. For the constant $\bar{r}$ method limits on error in V_S are about $\pm$ 5 dB so that for $|Z_{SC}|$ error limits are $\pm$ 8 dB. Note that the actual measurement errors are likely to be substantially smaller than these worst-case estimates of error *limits*.

III. RESULTS

A. Stability of preparation

In most of our experiments we made an initial measurement of the sound-pressure magnitude $|P_S|$ required to maintain a constant mean rate $\bar{r}$ over a range of frequencies.

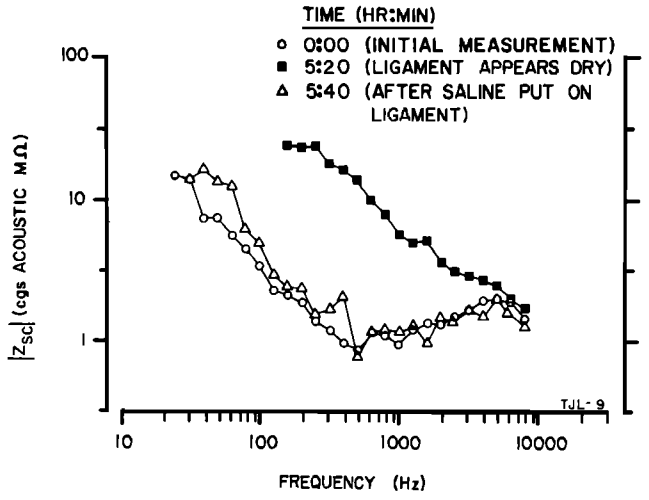

FIG. 7. Changes in the magnitude of the impedance of the stapes and cochlea Z_{SC} associated with drying of the annular ligament. The initial measurement was obtained with saline on the ligament. Approximately 5 h later $|Z_{SC}|$ had increased at most frequencies and the ligament appeared dry. After addition of a few drops of saline, $|Z_{SC}|$ returned nearly to its initial values.

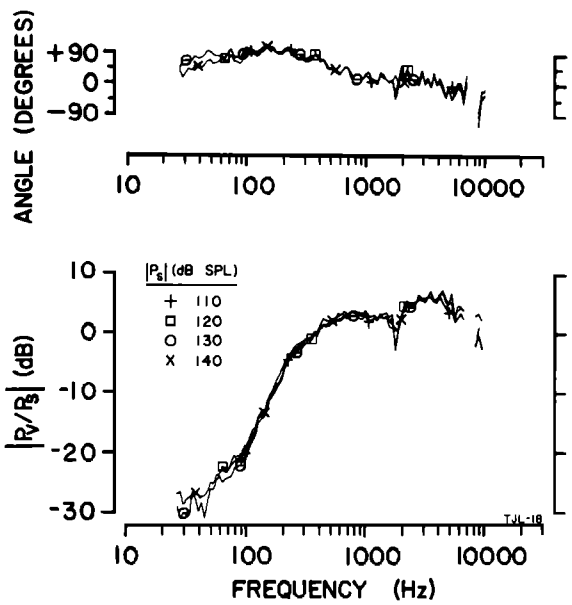

FIG. 8. Ratio of the pressure in the vestibule P_V to stimulus pressure P_S versus frequency with $|P_S|$ as a parameter. Neither the magnitude or angle shows significant dependence on stimulus level. Four curves are plotted in each section of the figure: one for each of the $|P_S|$ levels. Data points are evenly spaced on a logarithmic frequency scale with 40 points/decade. The symbols are used only to identify the curves. The sharp dips at 1800 Hz are an artifact which resulted from an instability in the acoustic system. No measurements were obtained in the region near 8 kHz because the stimulus source could not generate the specified $|P_S|$. For the data plotted above 8 kHz the upper magnitude points were obtained with $|P_S| = 110$ dB SPL; the data for 120 and 130 dB SPL are indistinguishable and they partially overlap with the points for 140 dB.

From these measurements the magnitude of the impedance of the stapes and cochlea $|Z_{SC}(f)|$ was computed. The "initial measurement" in Fig. 7 is typical of these results in that $|Z_{SC}|$ has a negative slope (about -6 dB/oct) for frequencies below 300 Hz and is approximately constant at a value near 1 MΩ for frequencies above 500 Hz.

In preliminary experiments the magnitude of $|Z_{SC}|$ often increased substantially over a few hours (Fig. 7). When this occurred, the stapes footplate and annular ligament appeared to be dry as seen through a dissecting microscope. The addition of a few drops of physiological saline to the exposed surface of the annular ligament usually resulted in the return of $|Z_{SC}|$ to approximately its original values (Fig. 7). Thus it seemed desirable to keep the tissue around the footplate moist at all times. Saline evaporated too quickly so mineral oil was used routinely in later experiments. If the oil disappeared or $|Z_{SC}|$ increased, more oil was added. This procedure resulted in measurements which were stable within a few dB over as long as two or three days in the living animal.

In one case, measurements of $|Z_{SC}|$ after death showed a gradual increase which reached 20 dB at low frequencies after 5 h even though the footplate was kept moist. No measurements from cadaver ears are included in this report.

B. Tests of linearity

In characterizing the system in terms of impedances [as in Eqs. (2) and (3)] we have assumed that the system is linear. Since it is difficult with the Mössbauer method to make accurate velocity measurements over a large dynamic range, measurements of P_V/P_S provide the most convenient method for measuring the dependence of a response on stimulus level. None of these measurements (e.g., Fig. 8) showed a significant deviation from linear growth of the fundamental component of P_V with increasing level of P_S. The velocity measurements were consistent with this conclusion in that linear growth of velocity was observed. For instance, the impedance magnitudes derived from both velocity-measurement methods were essentially equal (e.g., Fig. 16), even though the velocity magnitudes differed by 14 to 21 dB. Also, the waveforms of all the variables usually appeared to be sinusoidal; second and third harmonics for the velocity waveforms were at least 18 dB below the fundamental, and the p_S microphone and p_V transducer outputs appeared to be less distorted than the velocity waveforms. Thus we found predominantly linear behavior of responses at the stapes for stimuli $|P_S|$ up to 140 dB SPL.[2]

C. Effects of modifications of the system

In one cat the stapes was manually rocked back and forth so as to rupture most of the annular ligament with the stapes remaining in the oval window. The measured $|Z_{SC}|$ was smaller than normal for frequencies below 600 Hz and was essentially normal for frequencies above 600 Hz. This result and those obtained when the annular ligament was allowed to dry (Fig. 7) suggest that at low frequencies Z_{SC} is controlled by the annular ligament.

In some early experiments the lateral semicircular canal was inadvertently opened during the surgical preparation. $|Z_{SC}|$ in these preparations was generally lower than normal for frequencies between 1 and 10 kHz. This result suggests that in this frequency region Z_{SC} is determined by the cochlea; the hole provided a path for the stapes volume

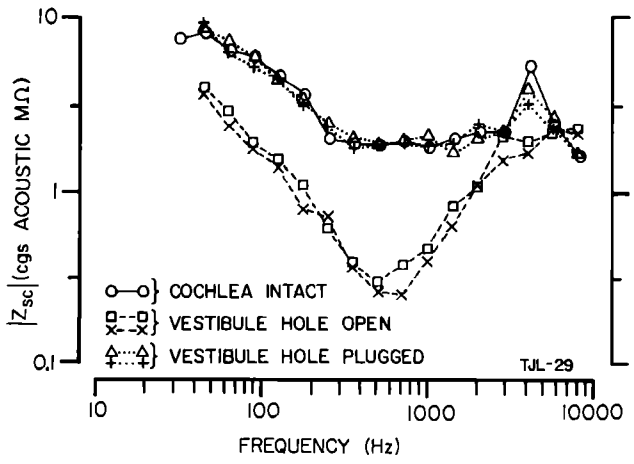

FIG. 9. The effect of a hole into the vestibule on the magnitude of the impedance of the stapes and cochlea $|Z_{SC}|$. Five curves are shown. The first was obtained with the cochlea intact (○), the second after drilling a hole (approximately 1/3 mm in diameter) into the vestibule (□), the third with a mechanical plug inserted into the hole (△), the fourth with the plug removed (×), and the fifth with it reinserted (+). The plug was held by a micromanipulator and could be quickly moved in or out of the hole. Seven hours elapsed between the first and second curve. For the second through fifth curves, approximately 20 min elapsed between successive curves. Similar results were obtained in another preparation in which the hole was repeatedly closed and opened using "Jeltrate" to form a gelatinous seal over the hole. The elevated value at 4 kHz is not typical (see Figs. 12 and 13) and did not appear in all the "intact" measurements for *this* animal.

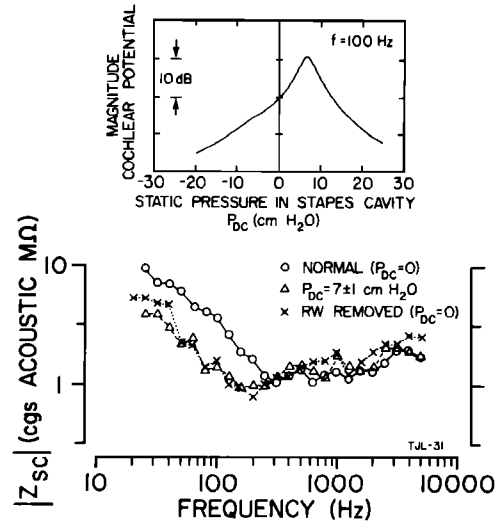

FIG. 10. Changes in the magnitude of the impedance of the stapes and cochlea $|Z_{SC}|$ associated with changes in static pressures on the stapes. The upper plot is cochlear-potential magnitude (|CP|) for $|P_S| = 130$ dB SPL at 100 Hz versus the static pressure in the stapes cavity P_{DC}. (A curve of similar shape was obtained for $|P_S| = 120$ dB.) CP was measured between a wire on the round window and the head holder. For these stimulus conditions |CP| was approximately 2μV rms when $P_{DC} = 0$. The lower plot is $|Z_{SC}|$ versus frequency for three static pressure conditions: $P_{DC} = 0$, the NORMAL experimental condition; $P_{DC} = 7 \pm 1$ cm H_2O, the value of P_{DC} that yielded the maximum |CP| in the upper plot; $P_{DC} = 0$ *and* the round-window membrane removed.

velocity which by-passed the cochlea and reduced $|Z_{SC}|$ by partially "short circuiting" the cochlear impedance. (Attempts to plug these holes were generally not effective; no further data from these preparations are included in our results.)

More systematic measurements of the effects of openings in the bony wall of the labyrinth were obtained when holes were drilled for insertion of a pressure probe. Results obtained with a hole drilled into the vestibule (Fig. 9) show that plugging the hole duplicates the "intact" condition and that the differences between the "open" and "plugged" conditions were repeatable. The reduction of $|Z_{SC}|$ for frequencies between 0.3 and 3 kHz with the hole open presumably results from the cochlear impedance being "short circuited" by the hole. The reduction in $|Z_{SC}|$ for frequencies below 0.3 kHz is more difficult to explain, since the impedance is supposedly determined by the annular ligament in this frequency range. Similar reductions in $|Z_{SC}|$ at low frequencies occurred when a hole was made in either the vestibule, scala tympani of the basal turn, or the round-window membrane.

To account for the low-frequency ($f < 0.3$ kHz) changes, it was hypothesized that the static perilymphatic pressure in the unopened labyrinth stretches the annular ligament so as to increase its incremental stiffness. To test this hypothesis, measurements were made with different static pressures in the cavity around the stapes. Stapes velocity was monitored by the Mössbauer average-rate method and also *changes* in velocity were detected by measuring changes in cochlear potentials recorded from the round-window membrane. With a fixed stimulus P_S at 0.1 kHz, a maximum in cochlear-potential magnitude (*and* in Mössbauer mean rate) occurred at a positive pressure of 7–8 cm H_2O (Fig. 10, upper). Subsequently, measurements (not shown) of |CP| versus static pressure were repeated after (a) opening a hole in the dura mater over the cerebellum so as to reduce cerebrospinal-fluid (csf) pressure and perilymphatic pressure and (b) removing the round-window membrane so as to reduce the perilymphatic pressure directly. These procedures produced a horizontal shift in curves such as Fig. 10 (upper) so that the location of the maximum moved toward zero pressure. In contrast to these results at 0.1 kHz, with $f = 1$ kHz only small changes (< 3 dB) in |CP| occurred with static-pressure variations. These results are consistent with the idea that pressure variations affect primarily the annular ligament, which controls Z_{SC} for the lower frequencies.

Measurements for three conditions (Fig. 10, lower) showed that $|Z_{SC}(f)|$ with the round-window membrane removed is approximately the same as that obtained when the round window is intact and a positive static pressure of 7 cm H_2O is applied on the lateral side of the stapes; at low frequencies $|Z_{SC}|$ under these two conditions is less than $|Z_{SC}|$ with the cochlea intact. These changes at low frequencies can be interpreted as resulting from static displacements of the stapes which produce changes in its incremental stiffness. When the static pressure difference across the annular ligament is zero (either from balancing the perilymphatic pressure with an external pressure or from reduction of perilymphatic pressure to zero), the stiffness of the annular ligament is a minimum. The magnitude of the pressure (7 cm H_2O) determined in this one cat is outside the range (11.4 to 18.0 cm H_2O) and only about 1/2 the mean value of csf and perilymphatic pressures reported for cat by Beentjes (1972).

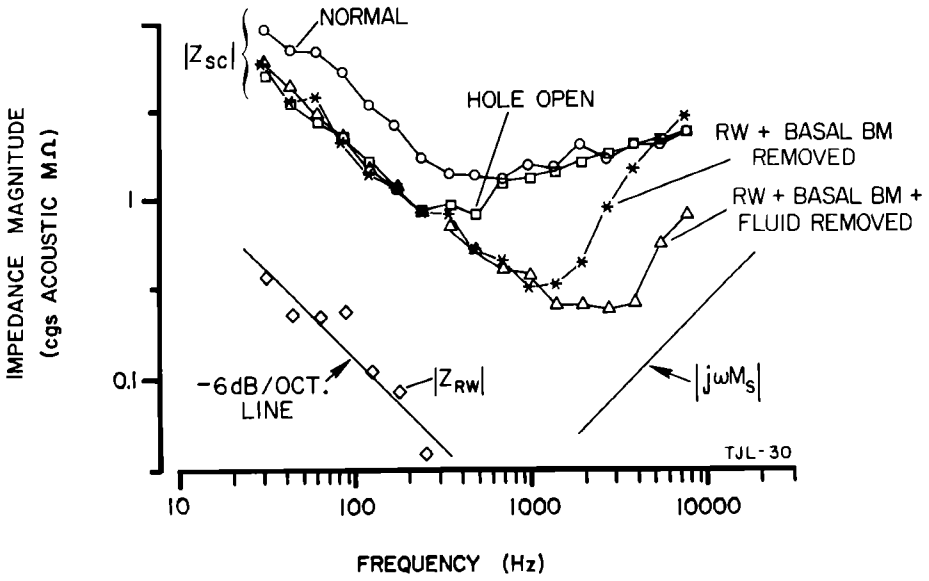

FIG. 11. Magnitude of the impedance of the stapes and cochlea $|Z_{SC}|$ for a series of cochlear manipulations. The initial measurement is labeled "NORMAL." A hole was then drilled into scala tympani near the round window and $|Z_{SC}|$ was determined with this "HOLE OPEN." A pressure transducer was inserted into the hole and sealed (measurement of $|Z_{SC}|$ under these conditions is not shown but is similar to the NORMAL measurement) and from pressure measurements in scala tympani (P_{RW}) the impedance magnitude of the round-window membrane was computed $|Z_{RW}| = |P_{RW}/U_S|$ (assuming $U_{RW} = U_S$). Next the round-window membrane and approximately 2 mm of the basal end of the basilar membrane were removed (RW + BASAL BM REMOVED) and $|Z_{SC}|$ was measured. Finally, aspiration of the perilymph in the basal region of both scalae yielded the "FLUID REMOVED" condition. The stapes was excised and weighed (wet weight = $M_S^m = 617\ \mu g$); the impedance of this mass is given by the curve $|j\omega M_S|$, where $M_S = M_S^m/A_{fp}^2$.

In two preparations (with similar results) more drastic modifications of the cochlea were carried out (Fig. 11). Opening a hole in scala tympani produced a decrease in $|Z_{SC}|$ for $f < 0.3$ kHz that is similar to the decrease produced by a hole in scala vestibuli (Fig. 9) or by removal of the round-window membrane. $|Z_{SC}|$ for $f > 0.6$ kHz was unchanged in this case because a scala tympani hole does not "short circuit" the cochlea as does a hole in the vestibule. Note that $|Z_{RW}| \ll |Z_{SC}|$. Since Z_{RW} was short circuited by the hole, subsequent removal of the round-window membrane probably did *not* appreciably alter $|Z_{SC}|$. However, removal of the most basal region of the basilar membrane reduced $|Z_{SC}|$ for $0.3 < f < 7$ kHz, indicating that the basilar membrane is normally an important factor in determining cochlear input impedance. When fluid was removed from the cochlea, $|Z_{SC}|$ decreased further for frequencies above 1 kHz indicating that the fluid alone provides a significant load on the stapes. With the fluid removed, $|Z_{SC}|$ at high frequencies ($f > 5$ kHz) is approximately three times the impedance of the measured stapes mass. The difference can be accounted for by the mass (equivalent to that of about 1 mm^3 of H_2O) associated with the added mineral oil and perilymph remaining on the footplate.

D. Impedance measurements

1. Impedance of the stapes and cochlea Z_{SC}

Z_{SC} magnitudes calculated from constant $\bar{r}$ data are shown in Fig. 12 for *all* experiments in which the measurement was made before opening the labyrinth. At each frequency the interanimal range of $|Z_{SC}|$ is about 10 dB and the frequency dependence is essentially the same in all cats. At frequencies below 300 Hz, $|Z_{SC}|$ has a slope of -6 dB/oct; for higher frequencies it is almost constant with a magnitude near 1.5 MΩ. In six of these 14 cats, we also obtained both the magnitude and the angle of Z_{SC} from measurements of p_S and v_S waveforms (Fig. 13). For frequencies below 0.3 kHz, where $|Z_{SC}|$ has a slope of -6 dB/oct, the angle approaches $-90°$. Near 1 kHz, $|Z_{SC}|$ is relatively constant and the angle is near 0°. Above 6 kHz the angle and magnitude tend to increase with frequency.

To determine how the stapes mass affects Z_{SC}, six stapes were removed after experiments, stored in saline, and

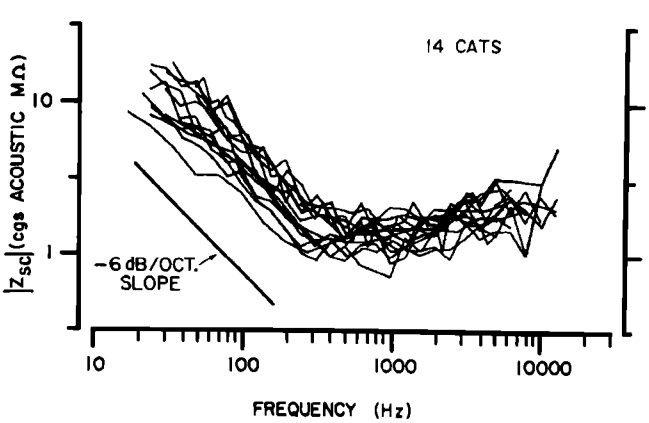

FIG. 12. Summary of measurements of the magnitude of the impedance of the stapes and cochlea $|Z_{SC}|$ made with the constant $\bar{r}$ method. In each curve data points are spaced evenly on a logarithmic frequency scale and are connected by straight-line segments. Point density varies among curves and is either 7, 10, or 20 points/decade.

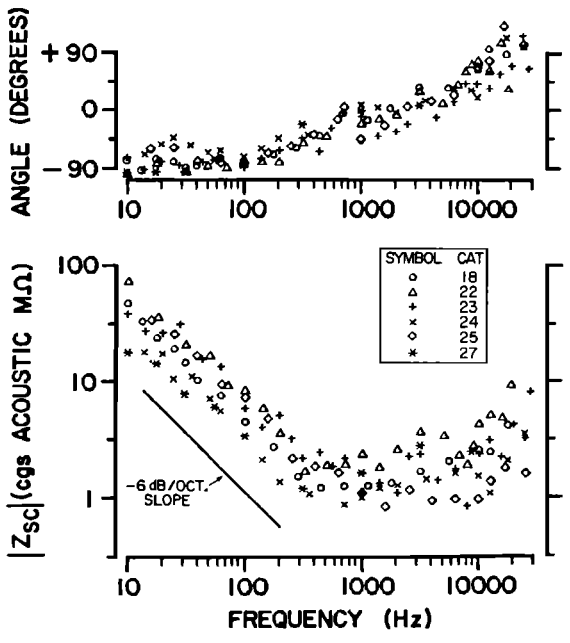

FIG. 13. Impedance of the stapes and cochlea Z_{SC} from six cats. Cat 25 is the only animal in this group in which a hole had been drilled into the vestibule before the measurements; $|Z_{SC}|$ measurements by the constant $\bar{r}$ method before the hole was made were close to those obtained after the pressure transducer was inserted and sealed into the vestibule.

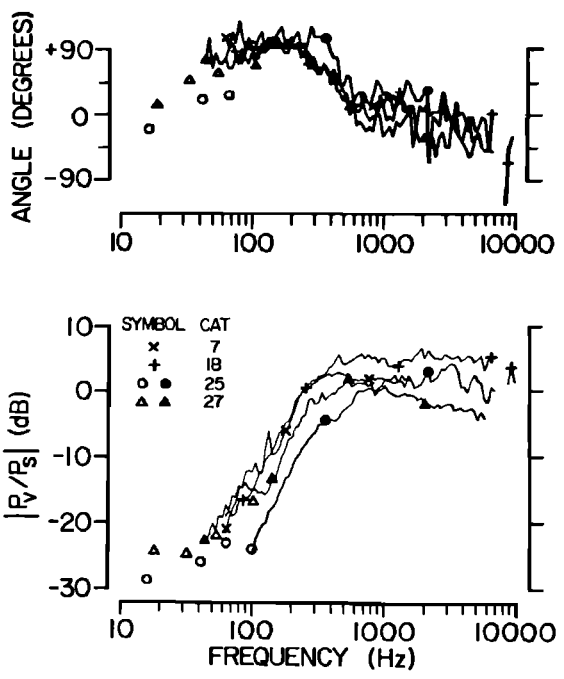

FIG. 14. Ratio of pressure in the vestibule to stimulus pressure P_V/P_S: measurements from four cats. The curves (marked by ×, +, ●, and ▲) are made up of straight-line segments connecting points with a density of 40 points/decade. The unfilled symbols at low frequencies represent data obtained from averaged waveforms for conditions where P_V was below the noise floor of the usual measurement system. Absolute calibrations of two transducers are involved in the determination of this pressure ratio. Because of possible errors in these calibrations, the magnitude of the ratio at middle and high frequencies may not be significantly different from 1 (0 dB).

weighed. The weight ranged from 422 to 618 μg with an average of 521 μg. This average value corresponds to an acoustic impedance magnitude at 10 kHz of 0.2 MΩ, which is about one tenth of $|Z_{SC}|$. Thus the mass of the stapes does not appear to contribute much to Z_{SC} even at high frequencies.

2. Cochlear input impedance Z_C

From measurements of P_V/P_S, Z_C can be computed by multiplying Z_{SC} by P_V/P_S. The P_V/P_S measurements shown in Fig. 14 are representative of those obtained from ten cats. The four cases shown are all those in which the effectiveness of the seal around the P_V probe was verified by measuring $|Z_{SC}|$ before and after the probe was placed in the vestibule. For frequencies above 1 kHz the magnitude is approximately constant near 0 dB and the angle varies around zero so that $P_V \cong P_S$. For $50 < f < 300$ Hz the magnitude decreases with frequency and the angle approaches + 90°. For frequencies below 50 Hz, $|P_V/P_S|$ is approximately constant at − 25 dB and the angle approaches 0°.

In one preparation we obtained measurements that were atypical in that $|P_V|$ was approximately equal to $|P_S|$ even at low frequencies. It was found that the cement base of the acoustic cavity around the stapes was not bonded to the bone in one spot anteroventral to the oval window. Since this region of the cement was in contact with sealant around the vestibule hole and pressure probe, apparently direct coupling of P_S to the pressure probe occurred through this pathway. Thus the rigidity of the enclosure around the stapes seems to be of great importance for the accuracy of P_V measurements. This kind of coupling was apparently not an appreciable factor in our reported P_V measurements, because we observed that, when drying of the annular ligament caused an increase in $|Z_{SC}|$, $|P_V/P_S|$ decreased.

Measurements of Z_C are shown in Fig. 15. At frequen-

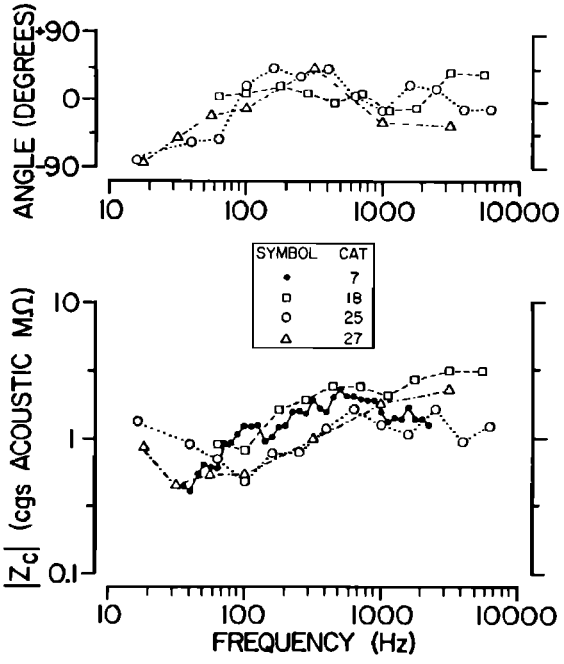

FIG. 15. Impedance of the cochlea Z_C from four cats. Magnitude and angle were determined from the product of Z_{SC} and P_V/P_S for three cats (18,25,27). For the fourth cat magnitude was determined from measurements of $|P_V|$ with $V_S|$ held constant.

cies below 50 Hz the data suggest that as frequency decreases the angle approaches $-90°$ and the magnitude increases. For frequencies between 50 and 500 Hz $|Z_C|$ increases with a slope of approximately 4 dB oct and the angle increases to a maximum value near $+45°$ and then decreases. For frequencies above 500 Hz, the angle averages about zero and the magnitude is approximately constant near $2M\Omega$.

3. Comparison of measurements

Figure 16 is a summary of Z_{SC} and Z_C measurements obtained in one animal utilizing both velocity-measurement methods. These results illustrate the agreement of the two methods of measurement and they allow comparison of Z_{SC} with Z_C.

The impedance magnitudes obtained from the two velocity-measurement methods agree within 4 dB. This is within the limits of error of the methods and is typical of the agreement obtained in all preparations. In this preparation results from both methods indicate that during the measurements there was a change in $|Z_C|$ at very low frequencies.

Comparisons of Z_{SC} to Z_C in other animals were similar in all cases. For frequencies below 0.3 kHz $|Z_{SC}|$ is greater than $|Z_C|$. For frequencies between 0.5 and 5 kHz $Z_{SC} \cong Z_C$. At the highest frequencies the angle of Z_{SC} tends to be more positive than the angle of Z_C. (An interpretation of the high-frequency differences between Z_{SC} and Z_C is presented in Sec. IV B3.)

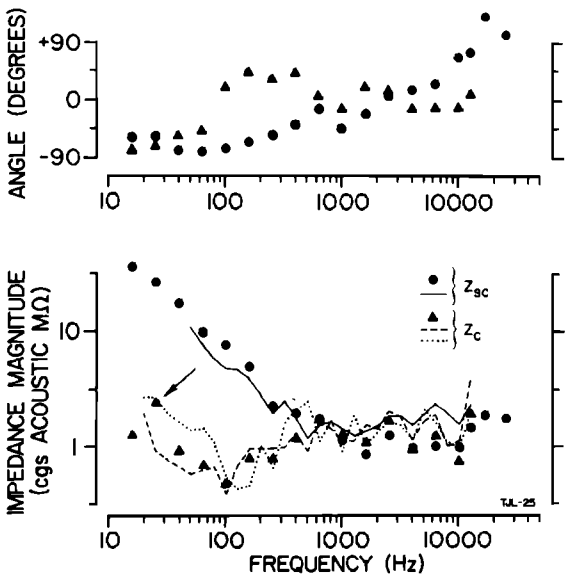

FIG. 16. Comparison of impedance results from one cat. Z_{SC} is the impedance of the stapes and cochlea; Z_C is the impedance of the cochlea. Filled symbols represent results obtained using velocity waveforms. The solid, dashed, and dotted curves are impedance magnitudes obtained with the constant $\bar{r}$ method. No symbols are plotted for these curves; points are equally spaced on a logarithmic frequency scale and are connected by straight-line segments. The dashed $|Z_C|$ curve was obtained before the waveform measurements. The dotted $|Z_C|$ curve was taken after 15 waveform data points were determined; the 15th data point (marked by an arrow) lies on the dotted curve. Thus a change in $|Z_C|$ at very low frequencies occurred during the time required for the waveform measurements. The other data points obtained in the latter part of this time interval were at higher frequencies, where significant changes in $|Z_C|$ did not occur.

IV. DISCUSSION

A. Comparison with previously reported measurements

1. Impedance of the stapes and cochlea Z_{SC}

The measurements of Z_{SC} in the cat reported by Tonndorf *et al.* (1966) and Khanna and Tonndorf (1971) also utilized acoustic stimuli delivered directly to the stapes. Tonndorf *et al.* (1966) used a capacitive probe to measure displacement of a region of the round-window membrane, whereas Khanna and Tonndorf (1971) used time-averaged holographic reconstructions to determine round-window volume displacement. The averaged results for $|Z_{SC}|$ from each of these studies are shown in Fig. 17 along with our averaged results. The most prominent differences occur at low frequencies where their values for $|Z_{SC}|$ are a factor of three to five larger than ours. Since we observed this kind of difference when the annular ligament was not kept moist (Fig. 7), it may be that some drying of the ligament occurred in their experiments.

The accuracy of the $|Z_{SC}|$ values obtained by Tonndorf *et al.* (1966) is limited by the assumptions that were used to convert their lineal displacement measurements to volume displacements. In their discussion of this problem Khanna and Tonndorf (1971, p. 1475) state that "all of these assumptions were rather poor." In addition, Tonndorf *et al.* (1966, p. 759) reported "some uncertainty" in the absolute calibration of the displacement measurements. These problems with the 1966 results (along with the presumed drying of the annular ligament) could easily account for the discrepancy between our average $|Z_{SC}|$ and theirs.

The holographic measurements (Khanna and Tonndorf, 1971) provided a description of the spatial distribution of round-window motion so that volume displacement could be obtained directly. However, in this study "variations between animals...were rather large" (Khanna and Tonndorf, 1971, p. 1480) as is shown by the $|Z_{SC}|$ range plotted in Fig. 17; Khanna and Tonndorf (1971, p. 1482) also reported that $|Z_{SC}|$ varied with stimulus level and time. Except for the changes that we found to be associated with drying of the annular ligament (Fig. 7) or with ineffective plugging of holes into the labyrinth, we have not encountered such variations. It seems likely to us that the reported variations with level and time, and interanimal variations resulted from inadequate control of experimental variables.[3] Their suggestion (Khanna and Tonndorf, 1971, p. 1482) that $|Z_{SC}|$ was altered by uncontrolled changes in csf pressure is not supported by our observations, since they report large variations in $|Z_{SC}|$ at 1.9 kHz, which is above the frequency range for which moderate static-pressure changes across the footplate alter $|Z_{SC}|$ (Fig. 10).

Møller's (1965) measurements of input impedance at the tympanic membrane in cat can also be used to estimate Z_{SC}, since he measured impedance before and after interruption of the incudo-stapedial joint. The circuit model of the middle ear shown in Fig. 18 indicates the assumptions involved in the computation. If it is assumed that (a) at all frequencies the ossicles move as a rigid body, (b) tympanic-membrane volume velocity that is not coupled to the malleus can be represented by a parallel admittance, and (c) possible

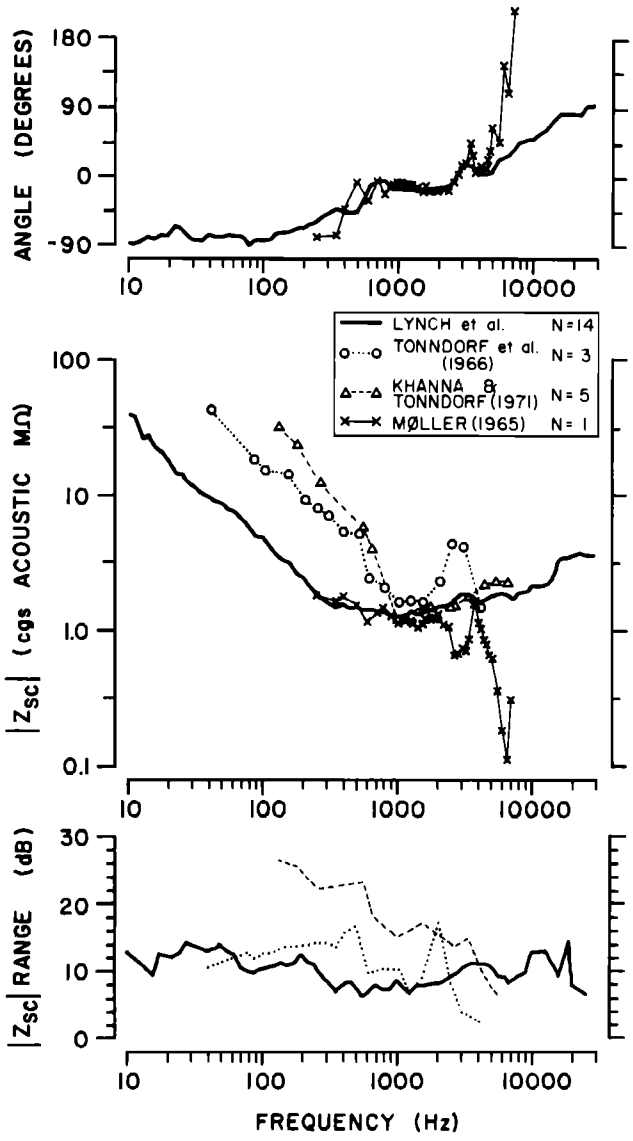

FIG. 17. Comparison of averaged measurements of impedance of the stapes and cochlea Z_{SC} in the cat. Our curves were obtained from the data shown in Figs. 12 and 13. Magnitude was computed using the points in Fig. 13 and data from Fig. 12 for those cats not in Fig. 13. Both magnitude and angle were computed by averaging all points in a 1/2 octave window whose center frequency was incremented in 40 steps per decade. The Tonndorf *et al.* (1966) curves are based on data for three cats shown in their Fig. 2. The Khanna and Tonndorf (1971) results are based on data in their Figs. 7 and 8. All their data from two live and three dead cats were included, because the measurements from the live cats tend to be the extremes, and the one preparation that is reported both in live and dead states shows little change. For both Tonndorf *et al.* (1966) and Khanna and Tonndorf (1971), averages were computed for each frequency of measurement. Intercat variability in the results from the three studies is indicated in the lowest plot. In Figs. 17, 19, and 20 "RANGE" is 20 log $|Z_{max}/Z_{min}|$: no attempt has been made to take account of the different number of cats involved in each study. RANGE was computed at all frequencies for which data existed for two or more animals; interpolation was used when necessary. In computing the impedance from Møller's (1965) results, data were taken from his Fig. 6 (Y_N, Y_{IJ}) and Fig. 8 (Y_{MB}) each containing results from one cat.

changes in the mode of motion of the ossicles and tympanic membrane that result from interruption of the incudo-stapedial joint or blocking of the malleus do not significantly alter Z_1, Z_2, and Z_{MB}, then the model of Fig. 18 is appropriate. Interruption of the incudo-stapedial joint replaces Z_{SC} with

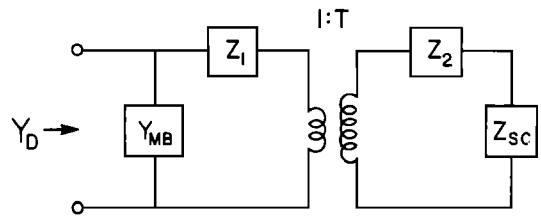

FIG. 18. A simple circuit model for the middle ear which was used to estimate the impedance of the stapes and cochlea Z_{SC} from Møller's measurements of admittance at the tympanic membrane Y_D. In this model voltage is analogous to sound pressure and current to volume velocity.

a short circuit. Thus

$$Z_{SC} = T^2[(Y_N - Y_{MB})^{-1} - (Y_{IJ} - Y_{MB})^{-1}], \qquad (7)$$

where the admittance at the tympanic membrane Y_D was measured for the following conditions:

$Y_D = Y_N$ = normal admittance,
$Y_D = Y_{MB}$ = admittance with the malleus blocked,
$Y_D = Y_{IJ}$ = admittance with incudo-stapedial joint interrupted, and
T = the effective transformer ratio.

The results of this computation with Møller's measurements of Y_N, Y_{MB}, and Y_{IJ} show (Fig. 17) that for $T = 60$ the estimated Z_{SC} agrees quite closely with our results for frequencies from 0.25 to 4 kHz. (For $f < 2$ kHz, $|Y_{MB}| < 1/4|Y_N| < |Y_{IJ}|$ so that Y_{MB} has little effect on the computed Z_{SC}. However, if the effect of Y_{MB} is not included, the estimated angle of Z_{SC} deviates appreciably from our measurements for frequencies from 2.5 to 4 kHz.) Above 5 kHz Z_{SC} estimated from Møller's results changes rapidly with frequency, unlike our measurements. It seems likely that Møller's measurements are relatively inaccurate in this frequency range (Lynch, 1981). In addition, if relative motion of the malleus and incus occurs, as has been reported in this frequency range by Guinan and Peake (1967), differences are expected at these frequencies, since the model of Fig. 18 is inadequate.

2. Ratio of pressure in the vestibule to pressure at the stapes $P_V/P_S = Z_C/Z_{SC}$

The ratio P_V/P_S was measured directly in our preparations (Fig. 14). Tonndorf and Khanna (1967) determined the pressure required outside the oval window to produce a given level of cochlear potential both with and without the stapes in place. The condition of equal cochlear potential should correspond at each frequency to equal volume velocity through the oval window, if the cochlea itself is unchanged by removal of the stapes. In that case, the ratio of pressures obtained in the two situations would be Z_C/Z_{SC} and should be the same as our measurements of P_V/P_S. Comparison of results (Fig. 19) indicates quite close agreement in that $|P_V/P_S|$ is near 0 dB for frequencies above 300 Hz, and has a positive slope (about 30 dB/decade) for frequencies between 50 and 300 Hz. The difference between the two sets of results increases with decreasing frequency for frequencies below 0.4 kHz. The source of this difference could again be drying of the annular ligament as suggested for the low-frequency differences in $|Z_{SC}|$ (Fig. 17).

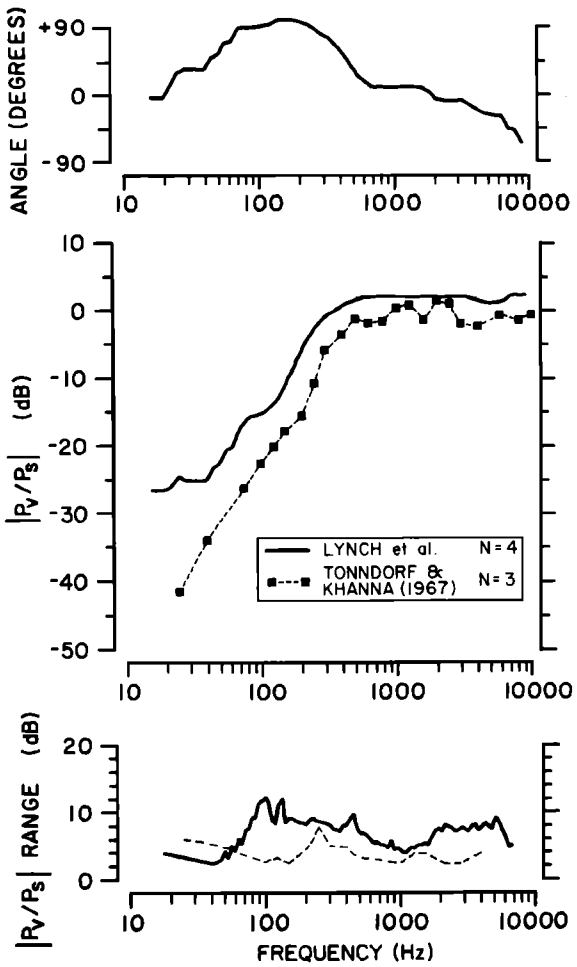

FIG. 19. Comparison of averaged measurements of the ratio of pressure in the vestibule to stimulus pressure P_V/P_S. Our curves were computed from the data of Fig. 14 by the following procedure: (1) all the points in Fig. 14 connected by straight-line segments were averaged (with a 1/2 octave window); (2) the "waveform points" (open symbols) which were at frequencies not included in the first average were averaged with a 1 octave window; (3) the two averages were then combined. The Tonndorf and Khanna (1967) curve is an average of data from three cats in their Fig. 10.

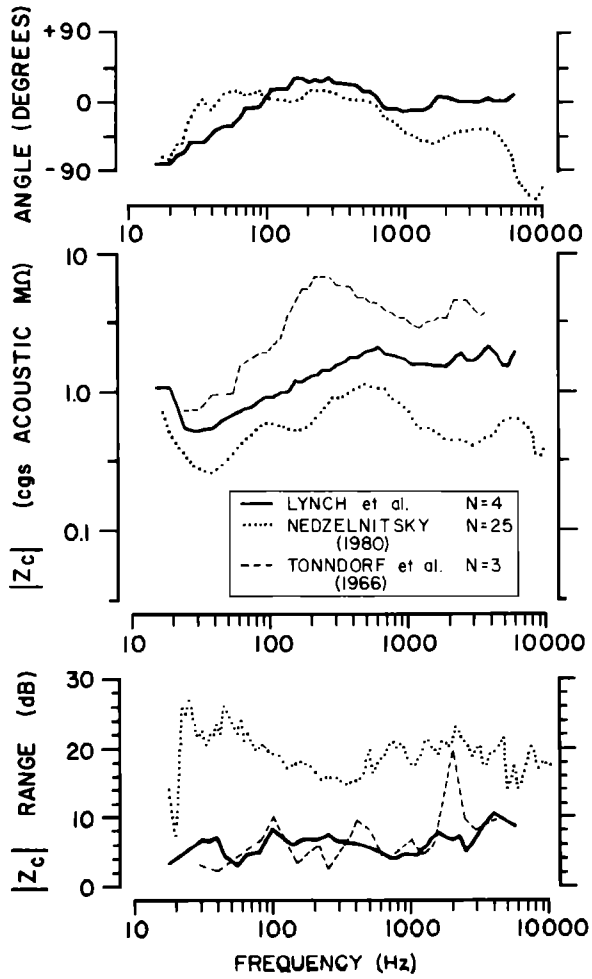

FIG. 20. Averages and ranges for measurements of cochlear input impedance Z_C from three studies in cat. Our curves are based on Fig. 15 of this paper. The curves for Tonndorf *et al.* (1966) were obtained from the data in Fig. 3 of that paper. In both cases data in a 1 octave window were averaged. Nedzelnitsky (1980) curves are medians of the magnitude and angle of $Z_V = P_{SV}/U_S$ from Fig. 16 of his paper. Note that for the Nedzelnitsky (1980) measurements the indicated RANGE is the range in measured pressure so that some of the variability may result from inter-animal variations in middle-ear transfer function rather than variations in $|Z_C|$.

3. Cochlear input impedance Z_C

Three sets of measurements are plotted in Fig. 20. The Nedzelnitsky (1980) curve (which was termed Z_V in that paper to distinguish it from Z_C) is based on measurements of sound pressure in scala vestibuli of the basal turn in 25 cats with intact ossicular chains. Measurements of stapes velocity were not made in these animals; Z_V was obtained by dividing the median pressure measurements by the average stapes volume velocity of Guinan and Peake (1967). Because Nedzelnitsky's pressure probes were placed 4–6 mm from the basal end of the basilar membrane, the measured pressure might be expected to differ from that at the stapes for high frequencies; Nedzelnitsky (1974a, p. 348) infers on theoretical grounds that for frequencies below 1 kHz, Z_V should not differ from the cochlear input impedance (Z_C) by more than about 2 dB in magnitude and 10° in angle. For frequencies below 1 kHz the principal difference between $|Z_V|$ of Nedzelnitsky (1980) and $|Z_C|$ measured by us is a frequency-*in*dependent difference of about 6 dB, which is within the estimated error limits of the two sets of measurements. If the Nedzelnitsky curve is translated upward by 6 dB the two curves are within 5 dB of each other over the frequency range from 15 to 2000 Hz. The frequency-independent difference could result from several factors including errors in the absolute calibrations of the pressure transducers and of the velocity measurement. Both sets of results indicate that at very low frequencies, $|Z_C|$ increases with decreasing frequency and the angle approaches $-90°$. This compliancelike behavior of Z_C occurs in the same frequency range where $|P_V/P_S|$ levels off (Fig. 19). Nedzelnitsky (1980) has proposed a model in which Z_C is controlled by the impedance of the round-window membrane in this frequency range.

The differences between our average $|Z_C|$ and the Tonndorf *et al.* (1966) average are probably *not* merely the result of interanimal variations, because at some frequencies the range of variation found in each series of measurements is less than the difference in the averages. Since these Tonndorf *et al.* (1966) motion measurements were made with a

capacitive transducer on the round window, the limitations on accuracy previously mentioned above could account for the differences.

The magnitude of cochlear input impedance in guinea pig has been inferred from measurements of intracochlear pressure and malleus motion by Dancer and Franke (1980, Fig. 2). Their results are similar to ours in that $|Z_C|$ is relatively independent of frequency (± 5 dB) over a broad frequency range. Also $|Z_C| = 0.45 \times 10^6$ dyn-s/cm^5 which is about one-half of our mid-frequency value. The positive slope of $|Z_C|$ vs f, which we have seen for $50 < f < 500$ Hz (Fig. 20), does not appear in the guinea pig results, which is consistent with the cochlear potential measurements of Dallos (1970). Further results from guinea pig (Franke and Dancer, 1980, Fig. 5) indicate that at frequencies below 20 Hz, Z_C behaves as a compliance, which is also similar to our results in the cat.

4. Input impedance across the cochlear partition Z'_C

If one considers the stapes volume velocity U_S as the input to the inner ear and the sound pressure in the vestibule, P_V as the response, then $Z_C = P_V/U_S$ is the transfer function. On the other hand, the input to the mechanical system of the inner ear (i.e., the cochlear partition) is presumably the *difference* in pressure between scala vestibuli and scala tympani at the basal end of the cochlea, $P_V - P_{RW} \triangleq P_C$, and the relevant transfer function is

$$Z'_C = (P_V - P_{RW})/U_S = P_C/U_S,$$

which we will call the input impedance *across* the cochlear partition.

Measurements from the basal turn of cat (Nedzelnitsky, 1980) indicate that for frequencies above 100 Hz the sound pressure in scala vestibuli is considerably greater than the sound pressure in scala tympani and therefore the pressure difference across the cochlear partition is approximately equal to the pressure in scala vestibuli. For this frequency range the input impedance $Z_C \cong Z'_C$. However, at frequencies below 40 Hz the pressures in scala vestibuli and scala tympani are nearly equal and Z_C is primarily determined by the round-window membrane impedance (Nedzelnitsky, 1980). To obtain Z'_C the round-window impedance must be subtracted, i.e., $Z'_C = Z_C - Z_{RW}$. (This approach has been described by Geisler and Hubbard, 1975.)

The measurements reported here do not permit us to determine Z'_C, since pressure was not usually measured in scala tympani. However, Nedzelnitsky (1980) has reported measurements of the ratio of pressure difference across the cochlear partition to sound pressure at the tympanic membrane, P_C/P_D. If this ratio is divided by the cat middle-ear transfer ratio, U_S/P_D, an estimate of Z'_C is obtained (Fig. 21). As mentioned above, the principal difference between Z'_C and Z_C (Fig. 20) occurs at frequencies below 40 Hz where Z_C is compliancelike [i.e., $Z_C \cong 1/(j\omega C_{RW})$], while Z'_C is more nearly masslike (i.e., $Z'_C \cong j\omega M_0$).

Masslike behavior for Z'_C at low frequencies was implied by studies of cochlear potentials in the basal turn of cats (Dallos, 1970; Weiss *et al.*, 1971), in which it was argued that cochlear microphonic potential (CM) is proportional to pressure difference (P_C) at low frequencies. The measurements of Dallos (1970) have been used to plot the ratio of basal turn CM to stapes volume velocity in Fig. 21.[4] As pointed out by Dallos (1974), the frequency dependence of these CM measurements parallels the Nedzelnitsky (1974b) pressure results quite closely. These results clearly suggest the masslike behavior.

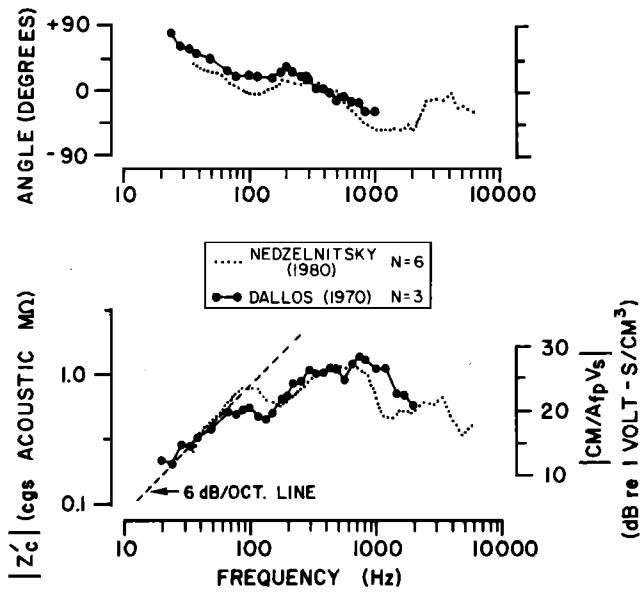

FIG. 21. Data relevant to the input impedance across the cochlear partition Z'_C. The Nedzelnitsky (1980) curves (left ordinate) are based on the median pressure difference from six cats (his Fig. 15). The Dallos (1970) curves (right ordinate) are based on medians of differentially recorded CM from the basal turn of three cats (his Fig. 3). In both of these studies acoustic stimuli were delivered to the tympanic membrane. The Guinan and Peake (1967, Fig. 14) average middle-ear transfer function was used to compute the ratios of the pressure difference and CM to stapes volume velocity. The vertical axes were positioned to approximately superimpose the plotted data.

In guinea pig, low-frequency masslike behavior of Z'_C is not indicated by CM measurements (Dallos, 1970); even for frequencies as low as 3 Hz (Franke and Dancer, 1980) the angle of Z'_C (though it is positive) does not approach 90°.

B. Network models for impedances

1. Goal

We have chosen mechanical network models to fit the impedance measurements of Sec. IV A. These networks describe the mechanical (or acoustic) system in terms of connected masses, resistances, and compliances. Since many middle-ear models (Onchi, 1949, 1961; Zwislocki, 1957, 1962, 1963; Møller, 1961) have been presented as electric circuit analogs of the mechanical system, we will also include electric circuits in which voltage is analogous to sound pressure and current is analogous to acoustic volume velocity. The two forms for the networks are completely equivalent: both are included as a convenience for readers with different backgrounds.

2. A simple network for the impedance of the stapes and cochlea Z_{SC}

The frequency dependence of the Z_{SC} measurements can be approximated by a three-element network (Fig. 22) in

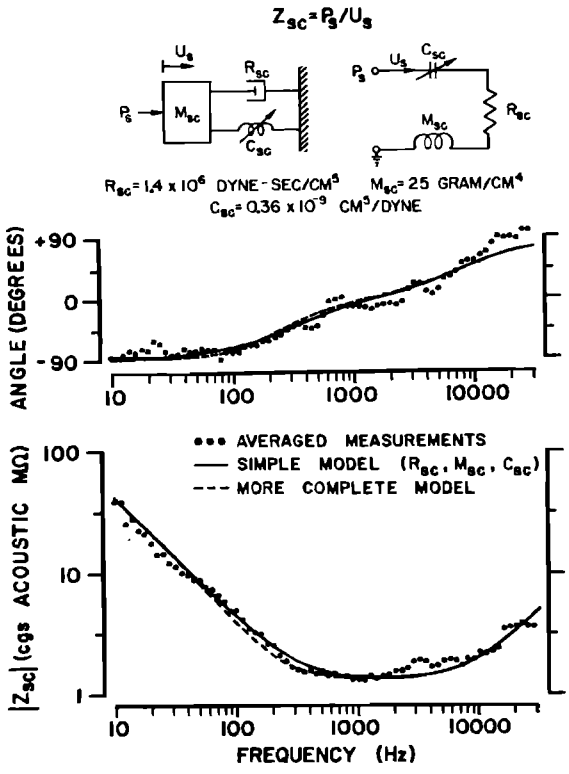

FIG. 22. Comparison of our averaged measurements of acoustic impedance of the stapes and cochlea Z_{SC} to the input impedance of a three-element network model. The averaged measurements are from Fig. 17. In Figs. 22, 23, and 24 networks are shown in two equivalent forms in the upper part of the figure with a mechanical diagram on the left and an electric circuit on the right. In both networks the labels represent acoustic variables and parameters (P_S,U_S; R_{SC},M_{SC},C_{SC}), which are analogous to either mechanical quantities (force, velocity; resistance, mass, compliance) or to electric quantities (voltage, current; resistance, inductance, capacitance). The arrows on the compliance elements indicate the dependence of this element value on static pressure difference across the stapes footplate. The maximum value of C_{SC} is presumably about three times larger than the value used here (Fig. 10). The dashed lines (which are visibly different from the solid for frequencies between 50 and 1000 Hz) indicate Z_{SC} for the more complete model shown in Figs. 23 (c) and (d).

which the compliance value C_{SC} is chosen to fit $|Z_{SC}|$ for frequencies below 0.1 kHz, the resistance value R_{SC} is chosen to fit $|Z_{SC}|$ for frequencies between 0.5 and 7 kHz, and the mass M_{SC} is chosen to fit for frequencies above 10 kHz. The root-mean-square (rms) differences (i.e., the mean over all the frequencies of the "AVERAGED MEASUREMENTS") between model and averaged measurements are 1.2 dB in magnitude and 12° in angle; the maximum differences at any frequency are 2.8 dB and 29°. Insofar as this model fits the Z_{SC} measurements, it provides a satisfactory description of Z_{SC} which should be adequate for modeling the normal middle ear.

The elements of this model can be associated primarily with either the stapes Z_S or the cochlea Z_C. Since we know that the annular ligament controls the low-frequency behavior of Z_{SC} (Figs. 7 and 10), C_{SC} must represent primarily the compliance of the annular ligament. Because destruction of the basal end of the basilar membrane and removal of perilymph reduces $|Z_{SC}|$ for frequencies above 0.3 kHz (Fig. 11), R_{SC} and M_{SC} must both be primarily determined by structures within the cochlea.

3. A more detailed network

Although the three-element network of Fig. 22 is adequate for representing the properties of Z_{SC}, it does not fully represent our knowledge of its components. Z_{SC} is the sum of the impedance of the stapes (and annular ligament) Z_S, the input impedance across the cochlear partition Z'_C, and the round-window membrane impedance Z_{RW} [Fig. 23(a) or (b)]. Our goal in this section is to represent each of these three impedances by a simple network of lumped elements such that the overall network has characteristics that mimic all the measurements. In a following section (Sec. IV C) we will relate the network elements to anatomical entities.

First we must choose representative sets of measurements to be matched by the network model. The averaged Z_{SC} results (Fig. 22) are taken as one set. For Z_C we have combined our measurements and those of Nedzelnitsky (Fig. 20) to give a grand average Z_C that is consistent with the Z_{SC} set (Fig. 24).[5]

The network used to represent the averaged sets of Z_C and Z_{SC} is shown in Fig. 23 [(c) or (d)]. After the circuit topology and element types were chosen to provide the main features in the Z_C and Z_{SC} curves, the element values were chosen as follows.

Consider first the impedance of the round-window membrane Z_{RW}. Nedzelnitsky (1980) has concluded that Z_{RW} behaves as a compliance for frequencies below 0.3 kHz. Assuming that $Z_{RW}=1/(j\omega C_{RW})$ we chose $C_{RW}=10\times10^{-9}$ cm^5/dyn to fit $|Z_C|$ for frequencies below 40 Hz where $Z_C\cong Z_{RW}$.

Consider next the impedance of the stapes Z_S. The measurements with perilymph removed from the cochlea (Fig. 11) indicate that Z_S is compliancelike up to 1 kHz, resistive for frequencies between 1 and 4 kHz, and masslike at higher frequencies. This indicates that Z_S can be represented by a three-element network of compliance, resistance, and mass. The compliance for our "normal" condition must be chosen so that when combined with C_{RW} the net compliance will equal C_{SC} (i.e., $1/C_{AL}=1/C_{SC}-1/C_{RW}$), which yields $C_{AL}=0.37\times10^{-9}$ cm^5/dyn. The stapes mass M_S is based on the average weight for excised stapes (0.52 mg) yielding an acoustic mass $M_S=M_S^m/A_{fp}^2=3.3$ g/cm^4. The resistance R_{AL} must be 0.2×10^6 dyn-s/cm^5 to yield the minimum value of $|Z_{SC}|$ (e.g., Fig. 11).

Consider now the elements necessary to represent Z'_C. The dominant element at mid-frequencies is R_C, which must be chosen such that $R_C=R_{SC}-R_{AL}=1.2\times10^6$ dyn-s/cm^5. To account for the masslike behavior of Z'_C at very low frequencies (Fig. 21) a parallel mass M_0 must be included; its value must be chosen to fit Z_C for frequencies between 50 and 100 Hz (Fig. 24) yielding $M_0=2250$ g/cm^4. The value for R_0 is chosen to match $|Z_C|$ near the frequency of its minimum (40 Hz). Since at high frequencies ($f>4$ kHz) $Z_S\cong j\omega M_S$, $Z_{SC}\cong j\omega M_{SC}$, and $Z_C\cong j\omega M_V$, $M_V\cong M_{SC}-M_S=25-3=22$ g/cm^4.

The behavior of the resulting eight-element network [Fig. 23 (c) or (d)] fits the averaged Z_{SC} and Z_C (and P_V/P_S) measurements quite well (Figs. 22 and 24, dashed lines). The rms differences are 1.2 dB in magnitude and 13° in angle for Z_{SC} and 1.2 dB and 16° for Z_C (2.0 dB and 24° for P_V/P_S).

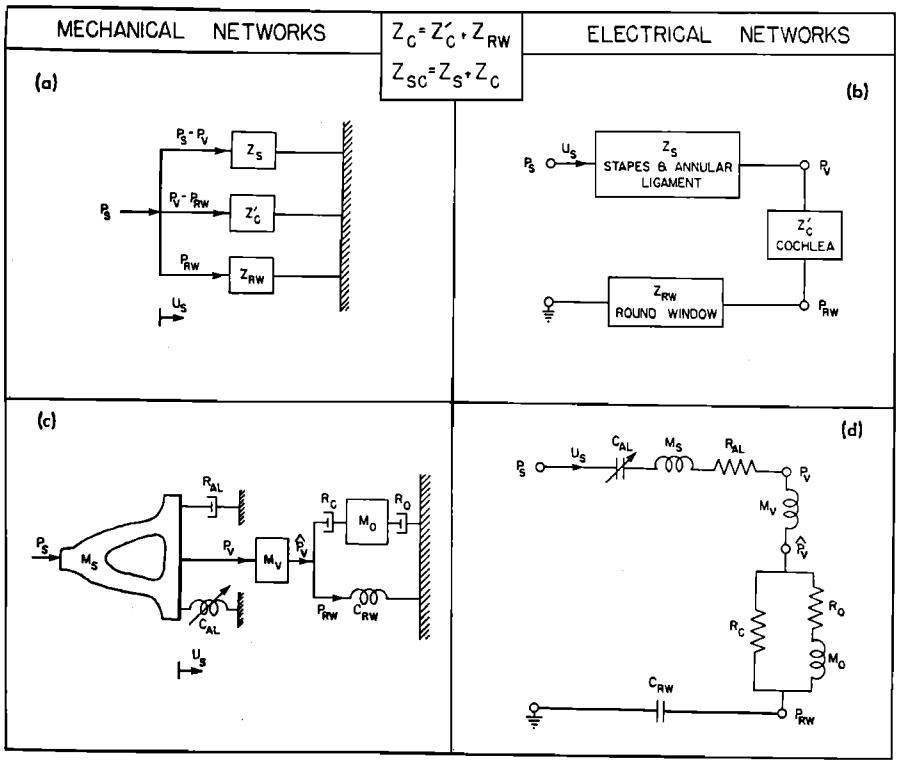

FIG. 23. Network representations of the impedance of the stapes and cochlea. The upper networks [(a) and (b)] indicate the relationship of the three main component impedances. The lower figures are the detailed networks that have been used to fit the measurements. Element values are $C_{AL} = 0.37 \times 10^{-9}$ cm^5/dyn, $M_S = 3.3$ g/cm^4, $R_{AL} = 0.2 \times 10^6$ dyn-s/cm^5, $M_V = 22$ g/cm^4, $R_C = 1.2 \times 10^6$ dyn-s/cm^5, $R_0 = 0.28 \times 10^6$ dyn-s/cm^5, $M_0 = 2250$ g/cm^4, $C_{RW} = 10 \times 10^{-9}$ cm^5/dyn.

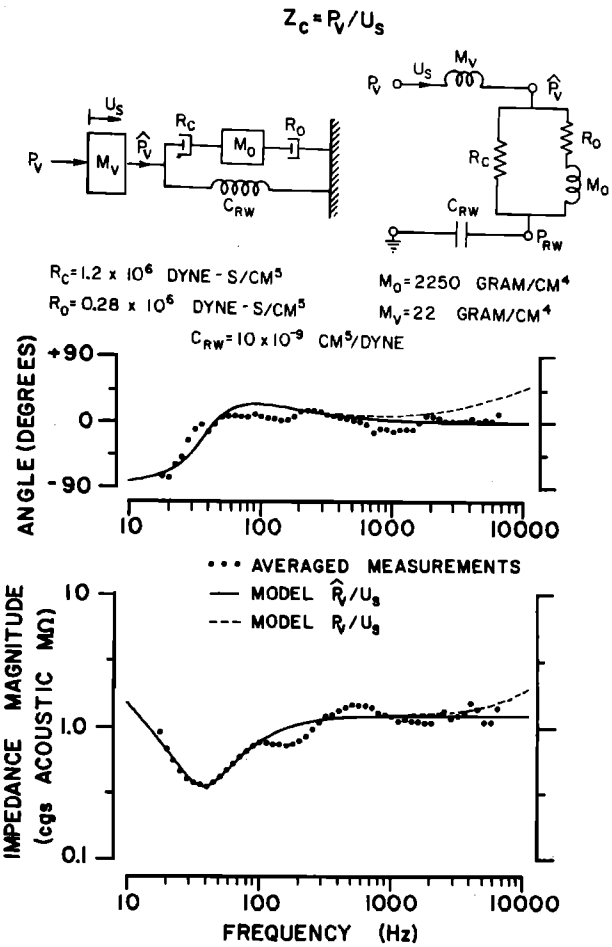

FIG. 24. Comparison of acoustic impedance of the cochlea Z_C from measurements and network model. The averaged measurements are those derived from the results presented in Fig. 20 (29 cats total). The networks in the upper part of the figure are the cochlear portions of those shown in Figs. 23(c) and (d). The solid curves are the model impedance $\hat{P}_V/U_S$, which excludes the mass M_V; the network impedance P_V/U_S (dashed curves) includes M_V.

The maximum differences at any frequency are 2.8 dB and 29° for both Z_{SC} and Z_C (5.9 dB and 66° for P_V/P_C).

There is an apparent disagreement between behavior of the network model and the measurements at high frequencies in that the angle of Z_C for the network (Fig. 24, P_V/U_S, dashed line) is significantly more positive than the averaged measurements (Fig. 24, dots). This suggests that M_V (which was needed in addition to M_S to account for the masslike behavior of Z_{SC} at high frequencies) should be a component of Z_S rather than of Z_C (which would change the Z_C model to the solid line in Fig. 24 with a reduction in rms differences to 1.1 dB and 11° and maximum differences to 2.8 dB and 27°). However, this suggestion conflicts with the results (Fig. 11) which show that $|Z_{SC}|$ is diminished at high frequencies by removal of perilymph. This conflict can be resolved if it is assumed that the pressure *measured* in the vestibule $\hat{P}_V$ differs from the actual pressure on the medial face of the footplate P_V (Ref. 6). Even though these two locations are separated by only a small fraction of a wavelength (for sound in water), there could be significant pressure differences. Since the stapes footplate covers only a fraction of the surface of the vestibule, some nonuniformity in the sound field will exist within the vestibule. We assume that this nonuniformity becomes significant at high frequencies and contributes a mass component (see Sec. IV C3). Thus M_V is interpreted as belonging to the cochlear input impedance, even though the measured Z_C does not appear to be masslike at high frequencies. In effect we assume that for high frequencies, P_S is a better estimate of the average pressure on the vestibular side of the stapes P_V, than the measured pressure $\hat{P}_V$.

C. Implications for structures that contribute to stapes impedance Z_S and cochlear impedance Z_C

This discussion is organized in terms of the elements of the network model of Fig. 23.

1. Stapes and annular ligament impedance Z_S

a. Annular ligament compliance C_{AL}. Our results indicate that between 10 and 1000 Hz, Z_S behaves as a compliance (Fig. 11) with the annular ligament being the structure that controls this behavior.

i. Effects of static perilymphatic pressure on middle-ear transmission. The demonstration (Fig. 10) that the incremental value of C_{AL} is sensitive to changes in the static pressure difference across the footplate suggests a mechanism through which pressure in the csf-perilymph system might affect middle-ear transmission. Measurements in the cat have demonstrated that changes in perilymphatic pressure tend to reduce the amplitude of cochlear potentials with the largest changes occurring for low-frequency stimuli (i.e., $f < 1$ kHz) (Allen *et al.*, 1971). This feature of these results is qualitatively in agreement with our proposed mechanism, since C_{AL} controls Z_{SC} only at low frequencies. It is difficult to make a more quantitative comparison because the smallest pressure used by Allen *et al.* is larger than the largest pressure that we used. However, it seems possible that, at least for moderate static pressures in the cat, a decrease of incremental annular-ligament compliance is the cause of a middle-ear transmission loss which secondarily causes a reduction of cochlear potential, rather than other mechanisms that have been proposed (Allen *et al.*, 1971, p. 393).

The proposed mechanism may also have significance for clinical studies that have demonstrated hearing loss associated with increased intracranial pressure (Saxena *et al.*, 1969). Following surgery to reduce the pressure, significant improvement in hearing occurred only for low frequencies (John *et al.*, 1979). Predictions of the influence of this mechanism in the intact ear are difficult because knowledge of the static strain of the annular ligament is lacking. The incus probably transmits some static force to the stapes which interacts with the perilymphatic pressure to determine the static strain of the annular ligament.

ii. Comparison of dynamic and static compliance. Kirikae (1959, p. 90) has reported measurements of static displacement of the stapes in excised temporal bones of cats. These results suggest an acoustic compliance of 0.16×10^{-9} cm^5/dyn. This value is about one-half of our average value for C_{AL} and about one-sixth of our value with no static pressure difference across the stapes footplate. However, the combination of the way in which Kirikae's mechanical load was applied, the post-mortem state of the ligaments, and the rather large displacement magnitude used could easily make the compliance estimates from his measurements smaller than our values. It seems possible that the differences are not significant and that the dynamic and static compliances of the annular ligament are equal for stapes displacements within the range associated with normal acoustic stimuli.

iii. Comparison to mechanical properties of other ligaments. Two properties of C_{AL} are similar to those of other ligaments, at least qualitatively: (1) Many kinds of connective tissue have nonlinear elastic behavior in which the incremental compliance decreases with increasing strain (e.g., Fung, 1967). (2) Stiffening of ligaments and tendons as a result of drying is well known from *in vitro* measurements (see Viidik, 1973, for review). Samples from bovine ligamentum nuchae show a compliance increase by a factor of almost 10^3 with an increase in water content from 0% to 60% (Gotte *et al.*, 1968). Our finding of changes by a factor of 30 with partial drying (Fig. 7) is well within this range.

Quantitative comparison of annular ligament elasticity to that of other ligaments can be attempted using results obtained with displacements that are small enough to yield linear behavior. To compare the different materials an elastic modulus (i.e., a characteristic of the ligament *material* which is independent of the ligament shape) is used. Measurements of ligament elastic properties made with a tensile stress in one direction yield values of Young's modulus (E = stress/strain) that vary over a considerable range. For the anterior cruciate ligament from the knee (of dogs) $E_{AC} = 10^9$ dyn/cm^2 (Haut and Little, 1969), whereas for the ligamentum nuchae from the neck (of cattle) $E_{LN} = 10^7$ dyn/cm^2 (Krafka, 1939; Carton *et al.*, 1962; Apter and Marquez, 1968; Yamada, 1970). The values for E are apparently correlated with the relative content of the fibrous proteins collagen and elastin. Ligaments that are relatively compliant contain mainly elastin and those that are stiffer are largely collagen (Hardy, 1951). For individual collagen fibers $E = 10^9$ to 10^{10} dyn/cm^2 (Harkness, 1961, p. 428; Stromberg and Wiederhielm, 1969), whereas for elastin fibers $E = 7 \times 10^6$ dyn/cm^2 (Carton *et al.*, 1962).

To estimate an elastic modulus for the material of the annular ligament we must make some assumptions about ligament configuration and stapes motion. If we assume (a) that the dimensions of the ligament are the same as the annular space between the edge of the footplate and the oval window, and (b) that stapes motion is purely translational in a direction perpendicular to the plane of the footplate, then the annular ligament is subjected to a pure shear stress. If we further assume that this material is homogeneous,[7] isotropic, and relatively incompressible, the compliance can be expressed[8] in terms of the dimensions of the annular space and Young's modulus E_{AL}:

$$C_{AL} = 3\omega A_{fp}^2/(tpE_{AL}), \tag{8}$$

where we have assumed that the thickness t and width w of the annular space are uniform over the whole perimeter p of the oval window. From Eq. (8), with dimensions $w = 20\,\mu$m, $t = 0.2$ mm, $p = 4$ mm (see Guinan and Peake, 1967, Fig. 11), $A_{fp} = 1.26$ mm^2, and $C_{AL} = 10^{-9}$ cm^5/dyn (where we assume that the unstressed C_{AL} is three times the value chosen for the network), we obtain $E_{AL} = 10^5$ dyn/cm^2. This result indicates that *if* the material which controls this compliance has the configuration of the annular space, the material is more compliant than anterior cruciate ligament by a factor of 10^4 and more compliant than ligamentum nuchae by a factor of 10^2.

It seems likely that erroneous assumptions may contribute significantly to the large discrepancy between apparent E_{AL} and E for other ligaments. Certainly the fibrous structure of the ligament would tend to make its elastic properties anisotropic. Probably more important is the likelihood that the mechanically significant components of the ligament may not be uniformly distributed; they may not even occupy

the annular space. Studies with specific stains indicate that the elastic tissue in human annular ligament is primarily on the vestibular and middle-ear surfaces of the footplate and extends on the surfaces of the bone for some distance from the annulus (Davies, 1948; Harty, 1953; Wolff and Bellucci, 1956). These inhomogeneities in the configuration of the ligament have not been described completely enough to be useful in making quantitative estimates of elastic moduli. However, it seems clear that if this configuration of the elastic tissue occurs in cat, the effective dimensions of the controlling structure would be much different from those of the annular space [i.e., in Eq. (8) w would be much larger and t smaller] and the actual modulus, E_{AL} could be much larger than that calculated above. Thus more precise determination of the configuration and composition of the annular ligament is required to make a meaningful comparison of annular ligament properties to those of other ligaments.

b. Annular ligament resistance R_{AL}. For frequencies between 1 and 4 kHz, Z_S is apparently resistive (Fig. 11). Although we have no direct evidence as to the structures involved in this effect, it seems likely that the annular ligament is the primary contributor. Apparently, properties of other ligaments have not been measured at frequencies in this range (Apter and Marquez, 1968).

c. Stapes mass M_S. We have measured an average stapes mass of 0.52 mg, which is the equivalent of an acoustic mass of 3.3 g/cm^4. Because this is considerably less than the equivalent mass of the stapes and cochlea ($M_{SC} = 25$ g/cm^4, Fig. 22), we conclude that responses of the normal middle ear in cats should not be sensitive to small changes in stapes mass.

2. Round window impedance Z_{RW}

Nedzelnitsky's (1980) results indicate that the impedance of the round-window membrane can be represented by a compliance for frequencies between 20 and 300 Hz and the results reported here (Fig. 11) support this conclusion. However, this representation may not be accurate for higher frequencies (Nedzelnitsky, 1974a). For lower frequencies we can use Kirikae's (1959, p. 89) measurements of static deflection of the round-window membrane in cat temporal bones to compute a compliance of 9×10^{-9} cm^5/dyn, which is approximately the value we have obtained. Perhaps the round-window membrane can be represented by a frequency-independent compliance for all frequencies below 300 Hz.

The visual appearance of the round-window membrane frequently changed during our experiments. The changes in $|Z_C|$ at low frequencies observed in one experiment (Fig. 16) can be interpreted as a decrease in C_{RW}. Nedzelnitsky (1974a, p. 151) also observed changes during some of his experiments that could be caused by a decrease in C_{RW}. Removal of periosteum from the surface of the cochlea could affect the vascular circulation to the outer round-window membrane with resultant changes in its mechanical properties. Such changes could easily have occurred without noticeable effect on our measurements, since the round-window impedance normally contributes little to Z_{SC} and only influences Z_C at very low frequencies.

3. Input impedance across the cochlear partition Z'_C

Some of the theoretical treatments of cochlear dynamics (Zwislocki, 1948; Steele, 1974; Geisler and Hubbard, 1972) predict that Z'_C is resistive and constant (for some range of frequency between 0.1 and 10 kHz) so that they are, in this respect, essentially consistent with our measurements. Other theoretical results have rather different behavior (Bogert, 1951; Fletcher, 1951; Dallos, 1970; Steele, 1974; Sondhi, 1978). (Most of these analyses were made to interpret results obtained on species other than the cat.) It should be possible to relate the elements of our descriptive network model to properties of cochlear structures through these models. In most of the studies of cochlear dynamics the relations are not evident upon inspection because computational methods were used to obtain solutions for a particular set of values for cochlear parameters. However, Zwislocki's (1948, 1965) analysis does yield a simple (approximate) expression for the dependence of Z'_C on cochlear properties [see also Sondhi (1981)].

a. Mid-frequencies, $Z'_C \cong R_C$. The result that Z'_C is approximated by a constant resistance over a rather broad frequency range ($0.1 < f < 3$ kHz) is consistent with some rather different views of cochlear mechanics.

It is sometimes suggested that the inner ear has a high input impedance because it is filled with a fluid having the acoustic properties of water; the acoustic impedance is then assumed to be that which would result from a uniform plane-wave propagating without reflection in an infinite tube (see Schubert, 1978, pp. 45–49, for some discussion of this issue). In this case $R_C = \rho c/A_{fp}$, where ρ and c are, respectively, the mass density and speed of sound for the cochlear fluid. Compelling *theoretical* reasons have been pointed out for rejecting this point of view (e.g., Wever and Lawrence, 1954, p. 381; Von Gierke, 1958; Killion and Dallos, 1979). First, since the cochlea is enclosed by bony walls giving it dimensions that (for the frequencies of interest) are only a small fraction of a wavelength of sound in water, it should *not* behave as an infinite tube. Second, in theoretical treatments of cochlear dynamics (e.g., Zwislocki, 1965; see Geisler, 1977, for review) the cochlear partition plays a key role in determining pressures and velocities in the cochlea, and therefore the mechanical properties of the partition should have an important influence on the input impedance. Our results add *experimental* evidence that conflicts with the view that $R_C = \rho c/A_{fp}$ in two respects: (a) the value we find for R_C is approximately one-tenth of $\rho c/A_{fp} = 1.2\times10^7$ dyn-s/cm^5 and (b) obliteration of the basilar membrane while leaving the fluid in the cochlea makes a large change in $|Z_{SC}|$ (Fig. 11). Thus, although the conception that the cochlear input impedance results from the wave impedance of the cochlear fluid alone *does* predict a constant resistance for Z'_C, the conception is demonstrably *in*correct.

The long-wave treatment of cochlear dynamics of Zwislocki (1965) yields the result that for a broad frequency range the acoustic impedance at a distance x from the basal end of the cochlea is closely approximated by

$$Z(x) = \{\rho/[S(x)C(x)]\}^{1/2}, \tag{9}$$

where $C(x)$ is the acoustic compliance per unit length of the

basilar membrane at the location x, and $S(x)$ is an effective area resulting from the areas of scala tympani S_t and scala vestibuli S_v i.e.,

$$S = S_v S_t/(S_v + S_t), \tag{10}$$

where both areas are evaluated at the position x. Zwislocki (1975, p. 46) argued that the available data from human, cat, and guinea pig were consistent with his theoretical impedance. Recently further results have been reported which allow computation of the variables in this expression.

In the cat, measurements of intracochlear pressure (Nedzelnitsky, 1980) and basilar membrane displacement (Evans and Wilson, 1975)[9] have been reported at the approximate location $x = 6$ mm. Ratios of these measurements (at 1 kHz) yield a "compliance" of 4×10^{-9} cm^3/dyn. To convert this to an acoustic compliance per unit length one must multiply by the effective width of the basilar membrane. The anatomical width at this location is 200 μm (Cabezudo, 1978). If we arbitrarily assume that the effective width is half this value, then $C(6\text{ mm}) = 40\times10^{-12}$ cm^4/dyn. The area of scala vestibuli at this location is about 7×10^{-3} cm^2 (Dallos, 1970) and scala tympani is somewhat larger, so we (somewhat arbitrarily) let $S(6\text{ mm}) = 5\times10^{-3}$ cm^2. With $\rho = 1$ g/cm^3 these values give an acoustic impedance of 1.6×10^6 dyn-s/cm^5. Thus, with these estimates of cochlear parameters, Eq. (9) gives an impedance at $x = 6$ mm that is about 1.3 times our R_C. One might try to evaluate Eq. (9) at $x = 0$ to find Z at the stapes footplate. Because the anatomy of the cochlea in the most basal region is quite different from the configuration usually assumed in the theoretical developments, it may not be useful to apply the formula in this way. Because (a) the volume velocity of the basal 6 mm of the basilar membrane is small relative to the volume velocity of the footplate (except at high frequencies) and (b) the perilymphatic scalae in this region are much larger than in more apical regions, the acoustic impedance at the footplate for frequencies below 1 kHz might be about the same as that at the 6 mm position [as theoretical estimates of Nedzelnitsky (1974b, p. 348) suggested]. Thus we conclude that the various mechanical measurements in the basal region of the cat cochlea are not inconsistent with Eq. (9) evaluated at $x = 6$ mm.

Results from mechanical measurements on guinea pigs can also be compared with evaluations of Eq. (9). From the basilar-membrane-displacement measurements of Wilson and Johnstone (1975, Fig.7), the pressure measurements of Dancer and Franke (1980, Fig. 2), and the basilar membrane-width measurements of Fernández (1952), one can estimate the compliance of the basilar membrane, $C(2\text{ mm}) = 40\times10^{-12}$ cm^4/dyn. With $S(2\text{ mm}) = 0.65$ mm^2 (Fernández, 1952) Eq. (9) yields $Z = 1.0\times10^6$ dyn-s/cm^5: about two times the value reported by Dancer and Franke (1980, Fig. 2). Again the predictions of Eq. (9) are larger than the experimentally determined $|Z_{SC}|$. However, the imprecisions involved in the measurements and computations are large enough that we can*not* conclude that Eq. (9) is *in*consistent with the measurements.

A better test of the validity of Eq. (9) would be to obtain accurate measurements in situations in which the cochlear parameters vary appreciably either across species or through experimental manipulation.

b. High frequencies, $Z'_C \cong j\omega M_V$. At high frequencies the behavior of Z'_C is approximately that of an acoustic mass M_V=22 g/cm^4. Zwislocki (1962, p. 1520) has suggested that a mass component in the cochlear impedance could result from "the column of perilymph between the oval window and the cochlea proper," and our interpretation of the Z_C and Z_{SC} measurements (Sec. IV B3) suggests that M_V results from the fluid near the footplate. If it is assumed that this mass results from a cylindrical plug of perilymph with the cross-sectional area of scala vestibuli at the basal end ($A_V = 2$ mm^2, Dallos, 1970, Fig. 10), the calculated length of this plug ($A_V M_V/\rho = 4$ mm) is much larger than the distance from the footplate to the basal end of the basilar membrane ($\cong 1$ mm). It is conceivable that because of nonuniform velocity distribution in the vestibule an additional mass component exists at high frequenices. Since the stapes drives a volume (the vestibule) which is larger in cross section than the footplate, a mass loading occurs (Burkhard and Sachs, 1977; Ingard, 1948). Because of the complicated shape of the vestibule it is difficult to estimate this effect quantitatively, but rough approximations indicate that this mechanism could introduce a mass effect of the right magnitude.

c. Low frequencies, $Z'_C \cong j\omega M_0 + R_0$. In our network model (Fig. 24) the pathway through R_0 and M_0 provides a low impedance for volume velocity from the oval window to the round window at low frequencies ($f < 100$ Hz). In discussions of cochlear mechanics it is usually assumed that the helicotrema provides such a pathway. A simple view of low-frequency cochlear dynamics might be that the volume velocity of the stapes is approximately equal to the volume velocity through the helicotrema with the volume velocity of the cochlear partition being relatively small. In this case the perilymph would flow primarily through a tube consisting of scala vestibuli, the helicotrema, and scala tympani. (A similar picture for low frequencies is indicated by Geisler and Hubbard, 1972). The considerations and calculations that follow are intended to test whether this view is compatible with the network element values required for R_0 and M_0.

Dallos (1970) considered various aspects of cochlear anatomy which might affect input impedance at low frequencies and he proposed a network model for Z_C that is identical in topology to the one that we have used for Z'_C (Ref. 10). We have, however, chosen quite different element values and our interpretation of the relative roles of the helicotrema and perilymphatic scalae is basically different. Dallos (1970) assumed that for low frequencies the cochlear input impedance is dominated by the impedance of the helicotrema. However, from our observations of unsectioned cat cochleas (embedded in epon and with the bony capsule removed) under a dissecting microscope, the helicotrema does not appear to be a dominant constriction in this path; the cross-sectional area of scala tympani in the most apical half-turn is not greatly different from that of the helicotrema. Also, the measurements reported by Dallos (1970, Fig. 10) show the area of scala vestibuli over its upper half to be only about two times the helicotrema area. Thus it seems likely that the impedance of this pathway can receive significant contributions

from the perilymphatic scalae.

From the dimensions of the helicotrema and scalae it should be possible to estimate the net impedance of this pathway. Unfortunately, the anatomical data are incomplete, and the lack of published measurements of scala tympani area is particularly bothersome, since the apical region of scala tympani is apparently the most constricted part of the path. If for a rough approximation we assume a circular tube with a radius of 125 μm,[11] the values of R_0 and M_0 that fit our measurements both require a tube length of approximately 7 mm.[12] In the cat a distance of 7 mm from the apical end of the basilar membrane encompasses the upper 1 and 1/2 turns of scala tympani (Schuknecht, 1960). Although perhaps only the upper half-turn of scala tympani has a cross-sectional area this small, the remainder of the pathway should also provide significant additions to the impedance. Thus the impedance of the perilymphatic tube could be approximately equal to $R_0 + j\omega M_0$. These calculations indicate that the values of M_0 and R_0 used in our network model could be consistent with a picture of flow at low frequencies which is primarily controlled by the perilymphatic tube.

D. Relationship of peripheral mechanical system to the threshold of hearing

The frequency-dependent transfer functions of the outer and middle ear and of the mechanical system of the inner ear must influence the frequency dependence of the behavioral threshold for tones. Rather contradictory conclusions have been reached on the relative importance of these components (Guinan and Peake, 1967, p. 1258; Dallos, 1973, p. 126; Zwislocki, 1975, p. 54; Khanna and Tonndorf, 1977; Franke and Dancer, 1980). In Fig. 25 physiological and behavioral data are plotted together so that the frequency dependence of behavioral threshold can be compared to relevant physiological variables.

The behavioral threshold measurements for the cat are plotted in terms of the sound-pressure level at the tympanic membrane P_D. Since we would like to make comparisons at frequencies below those at which the *cat* behavioral thresholds have been determined, a summary description of *human* low-frequency behavioral threshold measurements (Yeowart and Evans, 1974) is included.

From physiological data we have computed (for the intact middle ear) two estimates of the ratio P_D/P_C, where $P_C = P_V - P_T$ is the sound-pressure difference across the basal end of the cochlear partition. Our curve is based on mechanical measurements. The computation, $P_D/P_C = 1/[Z'_C(U_S/P_D)]$, was carried out using measurements of the middle-ear transfer function U_S/P_D and the averaged Z_C curve (Fig. 24), since $Z_C \cong Z'_C$. The Dallos (1970) curve is based on cochlear microphonic potential (CM) measurements with the assumption that CM is proportional to P_C (Dancer and Franke, 1980). These two estimates of P_D/P_C have the same frequency dependence for frequencies between 30 and 2000 Hz, thus supporting the assumption of proportionality of CM and P_C for low frequencies.

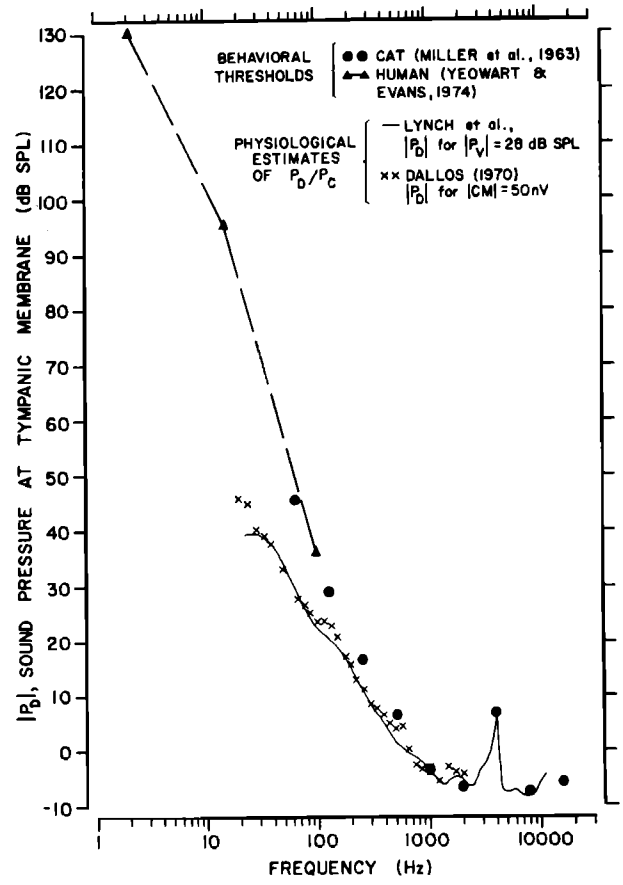

FIG. 25. Comparison of the frequency dependence of behavioral threshold and sound pressure at the input to the cochlea. Two sets of behavioral threshold measurements are summarized. Cat behavioral threshold data (monaural, Miller *et al.*, 1963, Table 3, p. 22) were modified by the transformation from free-field sound pressure to sound pressure outside the tympanic membrane (Weiner *et al.*, 1965, Fig. 7), so that the plotted points represent the sound pressure at the tympanic membrane (P_D) at behavioral threshold. The dashed line segments extending from 2 to 100 Hz summarize results for human subjects reported by Yeowart and Evans (1974); their binaural curve has been raised 3 dB to approximate the monaural threshold. Two estimates of P_D/P_C (P_C = pressure across the basal end of the cochlear partition) from physiological data are plotted. Our curve was obtained by combining the averaged $Z_C = P_V/U_S$ of Fig. 24 (using Z_{SC} for Z_C at the highest frequencies) with the closed-bulla middle-ear transfer function U_S/P_D from Fig. 21 of Guinan and Peake (1967) to give P_D/P_V. The Dallos (1970) data were taken from measurements of cochlear microphonic potential corrected (with Fig. 20 of Guinan and Peake, 1967) for the effect of opening the bulla and bony septum. The vertical positions of the two physiological measurements were chosen to make the points at 1 kHz coincide with the behavioral threshold. As a result, the $|P_D|$ for |CM| curve is for |CM| = 50 nV, and the $|P_D|$ for $|P_V|$ curve is for $|P_V|$ = 28 dB SPL.

Below 1 kHz it seems clear that the slopes of the behavioral and physiological results differ.[13] For frequencies between 20 and 100 Hz the physiological results behave approximately as f^{-2}, whereas the behavioral threshold data (two points for the cat and the line for human) are closer to f^{-3}. Thus, as frequency is lowered below 1 kHz, P_C at threshold increases; if we assume an extrapolation of the cat threshold parallel to the line suggested for human, P_C at behavioral threshold will be 38 dB larger at 20 Hz than at 1 kHz.

For frequencies between 1 and 8 kHz the behavioral and physiological data have approximately the same frequency dependence. [The sharp peak at 4 kHz is caused by a resonance in the middle-ear cavities (Guinan and Peake, 1967).] Thus behavioral threshold apparently corresponds to constant (i.e., within 3 dB) sound-pressure difference at the input to the cochlea in this frequency range.

At the high frequencies (i.e., 10 kHz and above) it is difficult to arrive at firm conclusions on the basis of available data. One problem is the relative lack of valid data. A second problem results from the uncertainties associated with the measurements of diffraction by the cat's head at these frequencies. Still another problem results from our interpretation of the apparent increase in $|Z_{SC}|$ at high frequencies. If this increase results from an impedance component contributed by the perilymph near the oval window, some of the associated pressure drop will not contribute to the pressure difference across the cochlear partition, and a component of Z'_C should be removed in calculations of P_D/P_C at high frequencies. Because of the uncertainties involved, we have not attempted to resolve this issue.

In summary, the idea that "behavioral sensitivity...(is) determined largely by the properties of the middle ear" (Dallos, 1973, p. 126) apparently holds for a restricted frequency range (perhaps 1 to 10 kHz for the cat). The results in Fig. 25 clearly indicate that the behavioral threshold at low frequencies is significantly influenced by more central mechanisms. Because the minimum characteristic frequency for auditory nerve fibers in the cat may be approximately 100 Hz (Liberman, 1978), one *would* expect threshold to increase below 100 Hz. Zwislocki (1975) has considered other mechanisms that might be involved. Since available evidence is quite incomplete, it is difficult to quantify the importance of different mechanisms.

To determine definitively why hearing sensitivity decreases at low and high frequencies it is necessary to obtain accurate measurements outside the frequency range that is usually thought of as "important" [as Yeowart and Evans (1974) have done]. Through understanding of the mechanisms that contribute to the loss of hearing sensitivity at the extreme frequencies, we may be able to understand how morphological variations are related to the frequency range of hearing for different species in both normal and pathological states.

ACKNOWLEDGMENTS

Professor L. Grodzins of the MIT Physics Department provided helpful advice on Mössbauer techniques. S. M. Liberman developed surgical techniques and made numerous other contributions. Others who have contributed are D. G. Beil, J. E. Bell, J. Cross, D. H. Johnson, M. C. Liberman, E. M. Marr, L. P. Miller, C. R. Northrup, W. M. Rabinowitz, M. D. Silverstein, and J. S. Wiley, III. Helpful comments on the manuscript were received from J. J. Guinan, Jr., N. Y. S. Kiang, W. M. Rabinowitz, J. J. Rosowski, and T. F. Weiss.

This work was supported in part by the National Institutes of Health and in part by the Research Fund of the American Otological Society. T. J. Lynch, III received support from the MIT Whitaker Health Sciences Fund and NIH Training Grants.

[1]It is easily demonstrated that the net force exerted by the pressure p_S acting over the middle-ear surface of the stapes is $A_{fp}p_S$. Consider the equilibrium condition obtained (neglecting gravitational forces) with the stapes subjected to a uniform pressure p_S over its *entire* surface. (Assume that the net force acting on the small fraction of the surface that abuts the oval window is negligible in this situation.) The surface integral of the force acting on the stapes can then be resolved into two components resulting from pressure (1) on the vestibular surface of the footplate and (2) on the middle-ear surface of the stapes. Since the stapes is in equilibrium, the net force exerted on the middle-ear surface is equal and opposite to that exerted on the vestibular surface, i.e., $A_{fp}p_S$.

[2]Although measurements reported here (Fig. 8) and those of Nedzelnitsky (1980) have indicated that intracochlear pressures grow linearly with stimulus sound-pressure level, neither study has investigated the prominence of distortion components of the kinds reported by Kemp (1978, 1979a, b) or Kim *et al.* (1980).

[3]We do *not* have data that directly disagree with the reported dependence of $|Z_{SC}|$ on sound-pressure level (Khanna and Tonndorf, 1971, Fig. 10) because we made no measurements at the high SPL's that they used (140–160 dB SPL at the stapes). However, the results of Nedzelnitsky (1980, Fig. 9) demonstrate linear growth of intracochlear sound pressure up to comparable levels (in a cat with intact ossicular chain).

[4]The Dallos (1970) measurements made with differential electrodes and those of Weiss *et al.* (1971) from micropipets in scala media are in essential agreement. The cochlear potential measurements of Tonndorf and Khanna (1967) from a round-window electrode exhibit a larger positive slope at low frequencies than the other data; this discrepancy could result from a significant neural component in their round-window records.

[5]The rationale and procedure for obtaining the grand average Z_C is as follows. We think that Z_C is nearly equal to Z_C for $f > 0.3$ kHz. There is a problem in deciding precisely how close the ratio $|Z_C/Z_{SC}| = |P_V/P_S|$ is to unity because the measured pressure ratio depends on the absolute calibration accuracy of two transducers. However, we can obtain an estimate from the measurements of Z_{SC} before and after removal of basilar membrane and cochlear fluid (Fig. 11). For the region where the angle of $Z_{SC} \cong 0$ (i.e., $1 < f < 4$ kHz), the average $|Z_{SC}| = 1.4$ MΩ; measurements with perilymph removed (averaged over two cats), indicate that $|Z_{SC}|$ has a value of about 0.2 MΩ in this frequency region. These figures lead to the conclusion that $|P_V/P_S| = |Z_C/Z_{SC}|$ is $(1.4 - 0.2)/1.4 = 0.86$ or -1.3 dB in this frequency range. However, in our averaged measurements (Fig. 19) $|P_V/P_S|$ is about $+2$ dB in this range. This small (i.e., 3.3 dB) inconsistency between the Z_{SC} and Z_C measurements probably results from the combined inaccuracies of the measurements. Because we have the least confidence in the P_V absolute calibration, we chose, somewhat arbitrarily, to make one adjustment in the absolute level of these measurements. We assumed that the average $|P_V|$ is too high by 3.3 dB and accordingly lowered the average $|Z_C|$ (solid curve, see Fig. 20) by this amount. We also raised the Nedzelnitsky curve by 2.5 dB to put it in agreement (on the average) with our shifted results for $f < 1$ kHz. The grand average (magnitude and angle) of the two sets of measurements is then computed weighting each according to the number of cats involved. Because theoretical estimates suggest that the Nedzelnitsky results differ significantly from the correct input impedance for high frequencies (see Nedzelnitsky, 1974a, p. 323), they were used only for $f < 0.7$ kHz.

[6]Section I defined P_V as the pressure acting over the vestibular surface of the footplate. However, succeeding sections have used P_V for the *measured* pressure in the vestibule. $\hat{P}_V$ is introduced here to denote *measured* pressure and to clarify the issues concerning M_V. This distinction is unnecessary for other discussions in this paper, and P_V is used for measured pressure in following sections.

[7]In the cat the annular space contains no fluid-filled articular cavities (Bolz and Lim, 1972) and it is apparently filled with fibers (Wolff and Bellucci, 1956).

[8]Equation (8) can be obtained simply. A pressure P acting on the stapes produces a shear stress $PA_{fp}/(tp)$. If the linear displacement is x, the shear strain is x/w (assuming $x \ll w$). Thus the shear modulus (shear stress/shear strain) is $n = wPA_{fp}/(tpx)$. The acoustic compliance, $C_{AL} = xA_{fp}/P$, can be expressed in terms of n as $C_{AL} = wA_{fp}^2/(tpn)$. For incompressible, iso-

tropic, homogeneous materials E is $3n$ (Fung, 1965, p. 131).

[9]There may be a problem with these Evans and Wilson measurements since they appear to show that the basilar-membrane displacement is relatively independent of frequency for constant sound pressure input to the ear. Measurements of cochlear potentials in cat indicate that basilar membrane displacement should be approximately proportional to frequency for frequencies between 0.2 and 1.0 kHz (Dallos, 1970; Weiss *et al.*, 1971).

[10]Dallos (1970) actually proposed his model to represent the *total* input impedance of the cochlea Z_C. In the absence of any intracochlear pressure measurements at that time he assumed that pressure in scala tympani was negligible and thus did not include the effect of the round-window membrane in his theoretical considerations. However, since his CM measurements are presumed proportional to pressure difference, these measurements should relate directly to Z_C'.

[11]M. J. Mulroy (1977), using scanning electron microscopic techniques, measured helicotrema diameters of $250 \pm 10\ \mu$m in two unsectioned cat cochleas; we assume that this diameter is roughly equal to that of the apical portion of scala tympani. [This helicotrema diameter is about half the value reported by Dallos (1970).]

[12] The "large tube" expressions, $R = L\,(2\mu\rho\omega)^{1/2}/(\pi a^3)$ and $M = \rho L\,[1 + (2\mu\omega/\rho a^2)^{1/2}]/(\pi a^2)$, are valid for $a(\rho\omega/\mu)^{1/2} \gg 1$. Both R and M depend on frequency but, since these elements influence Z_C predominantly in a small frequency range (40 to 100 Hz), we assume $\omega = 50/2\pi$. With $a = 125\ \mu$m, $\rho = 1$g/cm^3, $\mu = 10^{-2}$ g/cm-s (Steer, 1967; Money *et al.*, 1971), $\omega/(2\pi) = 50$ Hz, $a(\rho\omega/\mu)^{1/2} = 2.2$, which is not $\gg 1$ and therefore the "large tube" approximation is not accurate (Kinsler and Frey, 1950, p. 241). Nevertheless, it should be accurate enough for the rough approximation we seek. With $R = R_0 = 0.28 \times 10^6$ dyn-s/cm^5, and $M = M_0 = 2.25$ kg/cm^4, the R equation yields $L \cong 8$ mm and the M equation $L \cong 7$ mm.

[13]Zwislocki (1975) has come to the same conclusion from consideration of data obtained with human subjects.

Allen, G. W., Dallos, P., Sakamoto, S., and Homma, T. (**1971**). "Cochlear microphonic potential in cats. Effects of perilymphatic pressure," Arch. Otolaryngol. **93**, 388–396.

Apter, J. T., and Marquez, E. (**1968**). "A relation between hysteresis and other viscoelastic properties of some biomaterials," Biorheology **5**, 285–301.

Beentjes, B. I. J. (**1972**). "The cochlear aqueduct and the pressure of cerebrospinal and endolabyrinthine fluids," Acta Otolaryngol. **73**, 112–120.

Békésy, G. von (**1942**). "Über die Schwingungen der Schneckentrennwand beim Präparat und Ohrenmodell," Akust. Z. **7**, 173–186.

Békésy, G. von (**1960**). *Experiments in Hearing*, edited by E. G. Wever (McGraw-Hill, New York).

Bogert, B. P. (**1951**). "Determination of the effect of dissipation in the cochlear partition by means of a network representing the basilar membrane," J. Acoust. Soc. Am. **23**, 151–154.

Bolz, E. A., and Lim, D. J. (**1972**). "Morphology of the stapediovestibular joint," Acta Otolaryngol. **73**, 10–17.

Brüel, P. V. (**1964**). "The accuracy of condenser microphone calibration methods, Part I," Brüel and Kjaer Tech. Rev. No. 4, 3–29.

Brüel, P. V. (**1965**). "The accuracy of condenser microphone calibration methods, Part II," Brüel and Kjaer Tech. Rev. No. 1, 3–26.

Burkhard, M. D., and Sachs, R. M. (**1977**). "Sound pressure in insert earphone couplers and real ears," J. Speech Hear. Res. **20**, 799–807.

Cabezudo, L. M. (**1978**). "The ultrastructure of the basilar membrane in the cat," Acta Otolaryngol. **86**, 160–175.

Carton, R. W., Dainauskas, J., and Clark, J. W. (**1962**). "Elastic properties of single elastic fibers," J. Appl. Physiol. **17**, 547–551.

Dallos, P. (**1970**). "Low-frequency auditory characteristics: Species dependence," J. Acoust. Soc. Am. **48**, 489–499.

Dallos, P. (**1973**). *The Auditory Periphery. Biophysics and Physiology* (Academic, New York).

Dallos, P. (**1974**). "Comments," in *Facts and Models in Hearing*, edited by E. Zwicker and E. Terhardt (Springer-Verlag, New York), p. 54.

Dancer, A., and Franke, R. (**1980**). "Intracochlear sound pressure measurements in guinea pigs," Hear. Res. **2**, 191–205.

Dankbaar, W. A. (**1970**). "The pattern of stapedial vibration," J. Acoust. Soc. Am. **48**, 1021–1022.

Davies, D. V. (**1948**). "A note on the articulations of the auditory ossicles," J. Laryngol. Otol. **62**, 533–538.

Evans, E. F., and Wilson, J. P. (**1975**). "Cochlear tuning properties: Concurrent basilar membrane and single nerve fiber measurements," Science **190**, 1218–1221.

Fernández, C. (**1952**). "Dimensions of the cochlea (guinea pig)," J. Acoust. Soc. Am. **24**, 519–523.

Fletcher, H. (**1951**). "On the dynamics of the cochlea," J. Acoust. Soc. Am. **23**, 637–645.

Franke, R., and Dancer, A. (**1980**). "Cochlear microphonic potential and intracochlear sound pressure measurements at low frequencies in guinea pig," *Proceedings of the Conference on Low Frequency Noise and Hearing*, edited by H. Møller and P. Rubak (Aalborg, Denmark).

Fung, Y. C. (**1965**). *Foundations of Solid Mechanics* (Prentice-Hall, Englewood Cliffs, NJ).

Fung, Y. C. (**1967**). "Elasticity of soft tissues in simple elongation," Am. J. Physiol. **213**, 1532–1544.

Geisler, C. D. (**1977**). "Mathematical models of the mechanics of the inner ear," in *Handbook of Sensory Physiology, Vol. V/3 Auditory System, Clinical and Special Topics*, edited by W. D. Keidel and W. D. Neff (Springer-Verlag, New York), pp. 391–415.

Geisler, C. D., and Hubbard, A. E. (**1972**). "New boundary conditions and results for the Peterson–Bogert model of the cochlea," J. Acoust. Soc. Am. **52**, 1629–1634.

Geisler, C. D., and Hubbard, A. E. (**1975**). "The compatibility of various measurements on the ear as related by a simple model," Acustica **33**, 220–222.

Gilad, P., Shtrikman, S., Hillman, P., Rubinstein, M., and Eviatar, A. (**1967**). "Application of the Mössbauer method to ear vibrations," J. Acoust. Soc. Am. **41**, 1232–1236.

Gotte, L., Mammi, M., and Pezzin, G. (**1968**). "Some structural aspects of elastin revealed by x-ray diffraction and other physical methods," in *Symposium on Fibrous Proteins*, edited by W. G. Crewther (Butterworths, Australia), pp. 236–245.

Guinan, J. J., Jr., and Peake, W. T. (**1967**) "Middle-ear characteristics of anesthetised cats," J. Acoust. Soc. Am. **41**, 1237–1261.

Gundersen, T., Skarstein, Ø., and Sikkeland, T. (**1978**). "A study of the vibration of the basilar membrane in human temporal bone preparations by the use of the Mössbauer effect," Acta Otolaryngol. **86**, 225–232.

Hardy, R. H. (**1951**). "Observations on the structure and properties of the plantar calcaneo-navicular ligament in man," J. Anat. London **85**, 135–139.

Harkness, R. D. (**1961**). "Biological functions of collagen," Biol. Rev. **36**, 399–463.

Harty, M. (**1953**). "Elastic tissue in the middle-ear cavity," J. Laryngol. Otol. **67**, 723–729.

Haut, R. C., and Little, R. W. (**1969**). "Rheological properties of canine anterior cruciate ligament," J. Biomechanics **2**, 289–298.

Helfenstein, W. M. (**1974**). "Beitrag zur Messung der akustisch bedingten Bewegungen und Identifikation des mechanishen Teils der Innenohrs der Katze," thesis, Eidgenössischen Technischen Hochschule (Zurich, Switzerland) (unpublished).

Høgmoen, K., and Gundersen, T. (**1977**). "Holographic investigation of stapes footplate movements," Acustica **37**, 198–202.

Ingard, U. (**1948**). "On the radiation of sound into a circular tube, with an application to resonators," J. Acoust. Soc. Am. **20**, 665–682.

John, P. Y., Kacker, S. K., and Tandon, P. N. (**1979**). "Békésy audiometry in evaluation of hearing in cases of raised intracranial pressure," Acta Otolaryngol. **87**, 441–444.

Johnstone, B. M., Taylor, K. J., and Boyle, A. J. (**1970**). "Mechanics of the guinea pig cochlea," J. Acoust. Soc. Am. **47**, 504–509.

Johnstone, B. M., and Sellick, P. M. (**1972**). "The peripheral auditory apparatus," Q. Rev. Biophy. **5**, 1–57.

Kemp, D. T. (**1978**). "Stimulated acoustic emissions from within the human auditory system," J. Acoust. Soc. Am. **64**, 1386–1391.

Kemp, D. T. (**1979a**). "Evidence of mechanical nonlinearity and frequency selective wave amplification in the cochlea," Arch. Otorhinolaryngol. **224**, 37–45.

Kemp, D. T. (**1979b**). "The evoked cochlear mechanical response and the auditory microstructure—Evidence for a new element in cochlear mechanics," Scand. Audiol. Suppl. **9**, 35–47.

Khanna, S. M., and Tonndorf, J. (**1971**). "The vibratory pattern of the round window in cats," J. Acoust. Soc. Am. **50**, 1475–1483.

Khanna, S. M., and Tonndorf, J. (**1977**). "External and middle ears, the determinants of the auditory threshold curves," J. Acoust. Soc. Am. Suppl. 1 **61**, S4.

Killion, M. C., and Dallos, P. (**1979**). "Impedance matching by the com-

bined effects of the outer and middle ear," J. Acoust. Soc. Am. **66**, 599–602.
Kim, D. O., Molnar, C. E., and Matthews, J. W. (**1980**). "Cochlear mechanics: Nonlinear behavior in two-tone responses as reflected in cochlear-nerve-fiber responses and in ear-canal sound pressure," J. Acoust. Soc. Am. **67**, 1704–1721.
Kinsler, L. E., and Frey, A. R. (**1950**). *Fundamentals of Acoustics* (Wiley, New York), first ed.
Kirikae, I. (**1959**). "An experimental study on the fundamental mechanism of bone conduction," Acta Otolaryngol. Suppl. **145**, 1–111.
Krafka, J., Jr. (**1939**). "Comparative study of the histo-physics of the aorta," Am. J. Physiol. **125**, 1–14.
Lewis, G. K., and Peake, W. T. (**1971**). "System for displaying calibrated velocity waveforms of structures in the ear using the Mössbauer effect," M.I.T. Res. Lab. of Electronics, Q. Prog. Rep. **102**, 158–164.
Liberman, M. C. (**1978**). "Auditory-nerve response from cats raised in a low-noise chamber," J. Acoust. Soc. Am. **63**, 442–455.
Lynch, T. J., III, Nedzelnitsky, V., and Peake, W. T. (**1976**). "Measurements of acoustic input impedance of the cochlea in cats," J. Acoust. Soc. Am. Suppl. 1 **59**, S30.
Lynch, T. J., III (**1981**). "Signal processing by the cat middle ear: Admittance and transmission, measurements and models," Ph.D. thesis, M.I.T.
Miller, J. D., Watson, C. S., and Covell, W. P. (**1963**). "Deafening effects of noise on the cat," Acta Otolaryngol. Supp. **176**. 1–91.
Møller, A. R. (**1961**). "Network model of the middle ear," J. Acoust. Soc. Am. **33**, 168–176.
Møller, A. R. (**1965**). "An experimental study of the acoustic impedance of the middle ear and its transmission properties," Acta Otolaryngol. **60** 129–149.
Money, K. E., Bonen, L., Beatty, J. D., Kuehn, L. A., Sokoloff, M., and Weaver, R. S. (**1971**). "Physical properties of fluids and structures of vestibular appartus of the pigeon," Am. J. Physiol. **220**, 140–147.
Mulroy, M. J. (**1977**). Personal communication.
Nedzelnitsky, V. (**1974a**). "Measurements of sound pressure in the cochleae of anesthetized cats," Sc.D. thesis, M.I.T.
Nedzelnitsky, V. (**1974b**). "Measurements of sound pressure in the cochleae of anesthetized cats," in *Facts and Models in Hearing*, edited by E. Zwicker and E. Terhardt (Springer–Verlag, New York), pp. 45–53.
Nedzelnitsky, V. (**1980**). "Sound pressures in the basal turn of the cat cochlea," J. Acoust. Soc. Am. **68**, 1676–1689.
Onchi, Y. (**1949**). "A study of the mechanism of the middle ear," J. Acoust. Soc. Am. **21**, 404–410.
Onchi, Y. (**1961**). "Mechanism of the middle ear," J. Acoust. Soc. Am. **33**, 794–805.
Rhode, W. S. (**1971**). "Observations of the vibration of the basilar membrane in squirrel monkeys using the Mössbauer technique," J. Acoust. Soc. Am. **49**, 1218–1231.
Rhode, W. S. (**1978**). "Some observations on cochlear mechanics," J. Acoust. Soc. Am. **64**, 158–176.
Robles, L., Rhode, W. S., and Geisler, C. D. (**1976**). "Transient response of the basilar membrane measured in squirrel monkeys using the Mössbauer effect," J. Acoust. Soc. Am. **59**, 926–939.
Saxena, R. K., Tandon, P. N., Sinha, A., and Kacker, S. K. (**1969**). "Auditory functions in raised intracranial pressure," Acta Oto-laryngol. **68**, 402–410.
Schubert, E. D. (**1978**). "History of research on hearing," in *Handbook of Perception, Vol. IV, Hearing*, edited by E. C. Carterette and M. P. Friedman (Academic, New York).
Schuknecht, H. F. (**1960**). "Neutroanatomical correlates of auditory sensitivity and pitch discrimination in the cat," in *Neural Mechanisms of the Auditory and Vestibular Systems*, edited by G. L. Rasmussen and W. F. Windle (Thomas, Springfield, IL), pp. 76–90.
Sondhi, M. M. (**1978**). "Method for computing motion in a two-dimensional cochlear model," J. Acoust. Soc. Am. **63**, 1468–1477.
Sondhi, M. M. (**1981**). "The acoustical inverse problem for the cochlea," J. Acoust. Soc. Am. **69**, 500–504.
Steele, C. R. (**1974**). "A possibility for sub-tectorial membrane fluid motion," in *Basic Mechanisms in Hearing*, edited by A. R. Møller (Academic, New York), pp. 69–90.
Steer, R. W., Jr. (**1967**) "The influence of angular and linear acceleration and thermal stimulation on the human semicircular canal," Sc.D. thesis, M. I. T.
Stromberg, D. D., and Wiederhielm, C. A. (**1969**). "Viscoelastic description of collagenous tissue in simple elongation," J. Appl. Physiol. **26**, 857–862.
Tonndorf, J., Khanna, S. M., and Fingerhood, B. J. (**1966**). "The input impedance of the inner ear in cats," Ann. Otol. Rhino. Laryngol. **75**, 752–763.
Tonndorf, J., and Khanna, S. M. (**1967**). "Some properties of sound transmission in the middle and outer ears of cats," J. Acoust. Soc. Am. **41**, 513–521.
Viidic, A. (**1973**). "Functional properties of collagenous tissues," in *International Review of Connective Tissue Research, Vol. 6*, edited by D. A. Hall and D. S. Jackson (Academic, New York), pp. 127–215.
Von Gierke, H. (**1958**). "Discussion on process of sound conduction." Laryngoscope **68**, 347–354.
Weiss, T. F., Goldmark, G. M., Altmann, D. W., and Brown, R. M. (**1969**). "Automated system to control stimulus and measure response variables in experiments on the auditory system," M.I.T. Res. Lab. of Electronics Q. Prog. Rep. **95**, 122–127.
Weiss, T. F., and Peake, W. T. (**1972**). "Cochlear potential response at the round-window membrane of the cat—A reply to the comment of G. R. Price," J. Acoust. Soc. Am. **52**, 1729–1734.
Weiss, T. F., Peake, W. T., and Sohmer, H. S. (**1971**). "Intracochlear potential recorded with micropipets. III. Relation of cochlear microphonic potential to stapes velocity," J. Acoust. Soc. Am. **50**, 602–615.
Wever, E. G., and Lawrence, M. (**1950**). "The transmission properties of the stapes," Ann. Oto. Rhino. Laryngol. **59**. 322–330.
Wever, E. G., and Lawrence, M. (**1954**). *Physiological Acoustics* (Princeton U. P., NJ).
Wever, E. G., Lawrence, M., and Smith, K. R. (**1948**). "The middle ear in sound conduction," Arch. Otolaryngol. **48**, 19–35.
Wiener, F. M., Pfeiffer, R. R., and Backus, A. S. N. (**1965**). "On the sound pressure transformation by the head and auditory meatus of the cat," Acta Otolaryngol. **61**, 255–269.
Wilson, J. P., and Johnstone, J. R. (**1975**). "Basilar membrane and middle-ear vibration in guinea pig measured by capacitive probe," J. Acoust. Soc. Am. **57**, 705–723.
Wolff, D., and Bellucci, R. J. (**1956**). "The human ossicular ligaments," Ann. Otol. Rhinol. Laryngol. **65**, 895–910.
Yamada, H. (**1970**). *Strength of Biological Materials*, edited by F. G. Evans (Williams and Wilkens, Baltimore).
Yeowart, N. S., and Evans, M. J. (**1974**). "Thresholds of audibility for very low-frequency pure tones," J. Acoust. Soc. Am. **55**, 814–818.
Zwislocki, J. (**1948**). "Theorie der Schneckenmechanik," Acta Otolaryngol. Suppl. **72**, 76 pp.
Zwislocki, J. (**1957**). "Some impedance measurements on normal and pathological ears," J. Acoust. Soc. Am. **29**, 1312–1317.
Zwislocki, J. (**1962**). "Analysis of the middle-ear function. Part I: Input impedance," J. Acoust. Soc. Am. **34**, 1514–1523.
Zwislocki, J. (**1963**). "Analysis of the middle-ear function. Part II: Guinea-pig ear," J. Acoust. Soc. Am. **35**, 1034–1040.
Zwislocki, J. (**1965**). "Analysis of some auditory characteristics," in *Hand-Book of Mathematical Psychology, Vol. III*, edited by R. D. Luce, R. R. Bush, and E. Galanter (Wiley, New York), pp. 3–97.
Zwislocki, J. (**1975**). "The role of the external and middle ear in sound transmission," in *The Nervous System*, edited by D. B. Tower, *Volume 3, Human Communication and its Disorders*, edited by E. L. Eagles (Raven, New York), pp. 45–55.